



INNOVATIVE TOOLS FOR OFFSHORE WIND AND DC GRIDS

Deliverable 3.2 – Work Package 3:
**Report on dynamic converter interactions and the feasibility of
different software routines to represent the problems**

WP3 leader	KU Leuven
Dissemination level	Public
Website	http://innodc.org/
Grant Agreement number	765585
Due delivery	Month 18: 28 February 2019
Project dates	01/09/2017 – 31/08/2021

List of Contributors

Cardiff University	Wei Liu , <i>Jun Liang</i>
Elia System Operator	Nathalia de Moraes Dias Campos
KU Leuven	Vaishally Bhardwaj , <i>Jef Beerten,</i> <i>Dirk Van Hertem, Hakan Ergun</i>
Universitat Politècnica de Catalunya	Saman Dadjo Tavakoli , <i>Eduardo Prieto,</i> <i>Oriol Gomis</i>
U.Porto	Emily Maggioli , <i>Hélder Leite</i>

Early Stage Researchers (ESRs) in **bold**, supervisors in *italic*.

Summary

Power systems have been facing changes due to the introduction of renewable energy, distributed generation and HVDC connections between power systems and/or offshore wind farms. It is important to have an understanding of the dynamic interactions between the converters, which are the connecting elements between the AC and DC networks and their components. In order to improve the understanding of these interactions it is required to perform analysis from different perspectives of the network in different time frames, from stability to protection, including internal control loops of the converter. In this context this report will cover different tools used to study these interactions.

Contents

1	Introduction	5
2	AC Protection Case Study description: Integrating Converters in CAPE Software	6
2.1	CAPE Software	6
2.2	Modelling HVDC Converters in CAPE	8
2.2.1	Selected Model	8
2.2.2	Working Principles	8
2.2.3	Parameters and considerations	9
2.2.4	Limitations	10
2.3	Case Study description	11
2.3.1	Case study goals and considerations	11
2.3.2	Test network (for case study)	11
2.4	Conclusions	12
	References	13
3	DC protection studies using PSCAD software	15
3.1	Feasibility of PSCAD for dc protection studies	15
3.2	Introduction of PSCAD/EMTDC software	16
3.3	Modeling of an HVDC system in PSCAD/EMTDC	16
3.3.1	System modeling in PSCAD	17
3.3.2	Protection device modelling in PSCAD	19
3.4	Simulation results on dc protection in PSCAD	20
3.5	Conclusion	22
	References	23
4	Mutual Interactions and Stability Analysis of MMC-Based HVDC Link	25
4.1	Introduction	25
4.2	System Description	26
4.3	System Modeling	29
4.3.1	Modular Multilevel Converter (MMC)	29
4.3.2	MMC Control	30
4.3.3	HVDC Cable	31
4.4	System Linearization	32

4.4.1	MMC Linearization	33
4.4.2	Control System Linearization	33
4.4.3	Complete Linear Model	33
4.5	System Analysis	36
4.5.1	Eigenvalue Analysis	36
4.5.2	Sensitivity Analysis	37
4.5.3	Mutual Interactions	38
4.6	Conclusion	41
4.7	Appendix	41
References		43
5	AC transient stability interactions	46
5.1	Available software routines	47
5.2	Power system modelling	48
5.2.1	Synchronous generators	48
5.2.2	Converters	52
5.2.3	Transmission lines	55
5.3	Conclusions	57
References		58
6	Converter interactions in AC/DC grid operation	59
6.1	AC/DC converter interactions in multi-zonal systems	59
6.2	Computationally efficient implementation of AC/DC security constrained optimal power flow	62
6.3	Conclusion	64
References		65

1 Introduction

The new paradigm of the power systems require further investigations and studies on the dynamic interaction of its components. It is important to understand the different tools available for representing and studying these interactions. The focus in this work is the dynamic interactions with converters, the element connecting the AC-DC networks and offshore wind farms.

This report does not aim to provide an overview and comparison of all different software tools used for dynamic interaction studies with converters. It is rather the use of different softwares in specific applications (e.g. MMC, DC protections,...) for case studies, which is in line with the area of study of each of the contributing researchers. Each section will present the reasons for the selected software and its application to the area of study.

This report is organised into 5 chapters:

- **Chapter 2:** This section provides a case study outline using CAPE (common industry used tool for AC protections) to study the interaction between AC protections and the converter.
- **Chapter 3:** This section presents the feasibility of representing the converter in PSCAD and performing dynamic studies with DC protections.
- **Chapter 4:** This section provides a stability analysis of an MMC-based HVDC link using MATLAB Simulink.
- **Chapter 5:** This section covers available software tools for the study of AC transient stability analysis and modeling of a converter in some of these cases.
- **Chapter 6:** This section presents an overview of the converter interaction in AC/DC grid operation, presenting various tools and implementations used in these studies.

2 AC Protection Case Study description: Integrating Converters in CAPE Software

Written by Emily Maggioli, approved by Helder Leite.

This section presents a case study for the feasibility of the introduction of a VSC converter in CAPE software, allowing for future the studies on the dynamic interaction between the converter and AC transmission network protection. The work is organised into 4 sections:

1. Introduction to the tool, its main characteristics and justification for use;
2. Modelling approach proposed for the VSC based on its contribution to faults on the AC network;
3. Case study setup;
4. Main outcomes and proposed next steps.

2.1 CAPE Software

CAPE stands for Computer- Aided Protection Engineering and is a software developed for the engineers responsible for the protection of transmission and distribution networks [1]. This is a licensed software owned by Electrocon, which was recently acquired by Siemens [2].

The reason for using this tool is its applicability in the industry [3] [4], including the Portuguese TSO (Transmission System Operator) – REN. The electricity transmission grids are increasing in complexity, due to the increase of the integration of renewables, through the connection with large offshore windfarms and the interconnection of the grids from different countries (emergence of supergrids) [5]. This requires the protection engineers to consider increasingly complex networks and scenarios in order to assess and/or parameterize the protections of the grid. In this context, software like CAPE were created for modelling complex networks (which is can be a limitation for some tools) and use commercial relays in the testing, thus allowing a realistic analysis.

The focus in CAPE is the protection system, allowing for different testing options, such as [1] [6]:

- Relay Setting: Tool which supports initial parameter setting of the relays;
- Short-circuit: Simulation of faults (any type can be modelled) and network (no size limitations). This allows to confirm and adjust the short circuit level for equipment selection and settings;
- Power Flow: Considers that the load and generation are known values, from which it determines the steady state voltage on all the buses in the network through 2 possible algorithms, Newton or Fast Decoupled;
- System simulation: Testing environment, which allows the assessment of the whole system performance to a fault (realistic scenario). This is a stepped-event analysis as it allows the user to visualise the actions of the protection as it steps through the events until the fault(s) is(are) cleared.

In essence, CAPE does not allow for dynamic simulations, it treats each simulation as a series of steady states. This program is a phasor-based fault analysis program, which means it does not change the current or voltage over various cycles. In the case of short circuit analysis, the fault currents are assumed to be fixed until the breaker trips in a relay simulation. However, it is also a requirement to test the behaviour with respect to transient stability of the network. In this context CAPE-TS Link allows an interface between PSS®E [11] and CAPE for a dynamic simulation, which is accomplished as follows [14]:

- PSS®E provides the voltages to CAPE, that change dynamically at each time step;
- CAPE contains the detailed protection system;
- CAPE determines branch currents using the voltage information from PSS®E and combines with its own zero- and negative-sequence networks, evaluating the relay operation. If there is a breaker operation, then this information is passed on to PSS®E, at each time step.

- Simulation ends once it reaches the defined simulation time or by user action.

Other than the integration above, to this moment, this tool does not allow for user-imbedded code, except in the Macro section using “CUPL” language with CAPE commands [3].

2.2 Modelling HVDC Converters in CAPE

2.2.1 Selected Model

For the purpose of this work, the converter considered is a VSC (Voltage Source Converter), a common converter which is integrated in the networks, replacing the previously established LCC technology [7].

In CAPE it is only possible to model the AC network and/or AC terminals [9]. For protection studies, the interest is the contribution of the converter to a fault on the AC network. Thus, the proposal made for modelling a VSC is to consider the converter as a type 4 wind generator because the converter contributes with balanced or positive-sequence currents for all fault types [8] [9].

The category - 4 generator has a variable-speed synchronous generator and a power converter that converts wind-generated power to the system frequency [8] (see Figure 1).

2.2.2 Working Principles

This type of generator has the ability to maintain the rated power and allows the current to vary up to its limit in order to maintain the specified power [9]. Similarly, to what happens in wind farms, it is designed to ride-through voltage dips, keeping the source connected and will cause the current to persist until the fault is cleared. The inverter electronics allows only positive sequence current to be generated, and it is always maintained in synchronism with the positive sequence voltage [8] [9].

In CAPE’s steady-state models, a similar approach is observed as in other phasor-based fault programs; the computed fault currents are assumed to

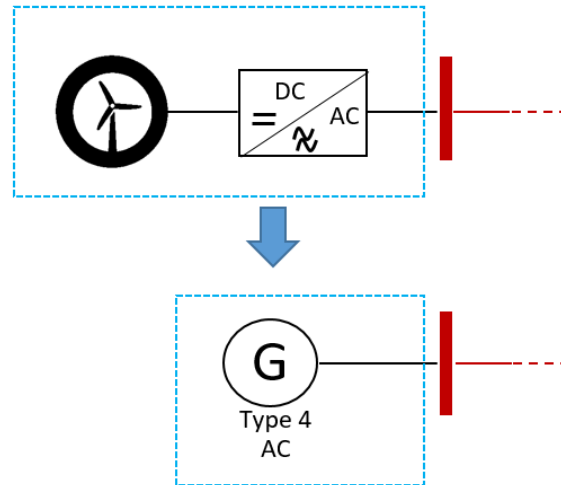


Figure 1: Converter model simplification in CAPE

be fixed until a breaker trips in a relay simulation. The steady-state fault calculation does not account for dynamic effects within machines that may reduce the current after a few cycles. CAPE therefore predicts the worst case, with higher breaker currents and faster protective device operations than actually occurring [9].

CAPE treats generators as a synchronous generator with appropriate sub-transient sequence impedances. Transient and steady-state impedances are also available in the database.

While the current is below the limit, the power and power factor angle are maintained by the converter.

2.2.3 Parameters and considerations

The parameters available, which are specific to the category – 4 generator, are as follows [9] [6]:

- Current limit
 - Maximum current under fault condition the converter will maintain the power and power factor angle;
 - A typical value is 1.1 p.u. (which is equivalent to saying $1.1 \times I_{MachineBase}$);
- Rated MVA

- Given total rated power output;
- Rated kV
 - AC output voltage at the generator side;
- Operating voltage:
 - Minimum and maximum operating voltage;
 - The current supplied will be zero if the voltage is below the minimum;
 - Typical values are $[0.15 ; 0.9] = [\text{min}; \text{max}]$;
- Power factor [degrees]:
 - This is the target value for phase lead of the bus from the current from the generator to the network;
 - -90° for a generator absorbing reactive power;
 - $+90^\circ$ for a generator delivering reactive power;
 - 0° if the current and voltage are in phase and delivering real power;
 - Typical value $=\arccos(0.95)=18^\circ$;
- Time constant [seconds]
- Ground connection

There are also some additional parameters and considerations, more generator specific, which can be modified for a better behaviour, such as:

- Power flow
- Impedance (short circuit)

2.2.4 Limitations

At a first observation and use of the tool, there could be a limitation with regards to harmonic contribution from the converter and also any contribution from the DC side, as CAPE only considers AC.

Another limitation could be the integration with other tools, as it does not allow for user-embedded code, However, for dynamic studies there is the possibility of the integration with PSSE, which requires a further understanding. [3].

ANSI No.	Description
21	Distance relay
25	Synchronizing or synchronism-Check Device
50	Instantaneous over-current
50N	Neutral instantaneous over-current
50BF	Breaker failure
51	Ac Time over-current relay
81	Frequency relay
85	Carrier or pilot-Wire receiver relay - teleprotection
87	Differential

Table 1: ANSI numbers for Line Protection

2.3 Case Study description

2.3.1 Case study goals and considerations

This section describes the case study setup. The goal is to define a test network with AC network protections and HVDC connections (converter end), to allow preliminary testing and to confirm some of the behaviour described in existent reports such as [7] [5]. The network described is a simplified representation, as a starting point before moving on to more complex network layouts (real networks).

2.3.2 Test network (for case study)

The test network is a simplification of the AC network and a consideration of the main components in a DC-AC connection, based on [7]. Each relay or Protection Unit (PU) is associated to a specific component like transformer, line, among other, and each PU has various functions associated, which are standardized as ANSI numbers [13] [12]. The meaning of these functions mentioned below are summarized in Table 1.

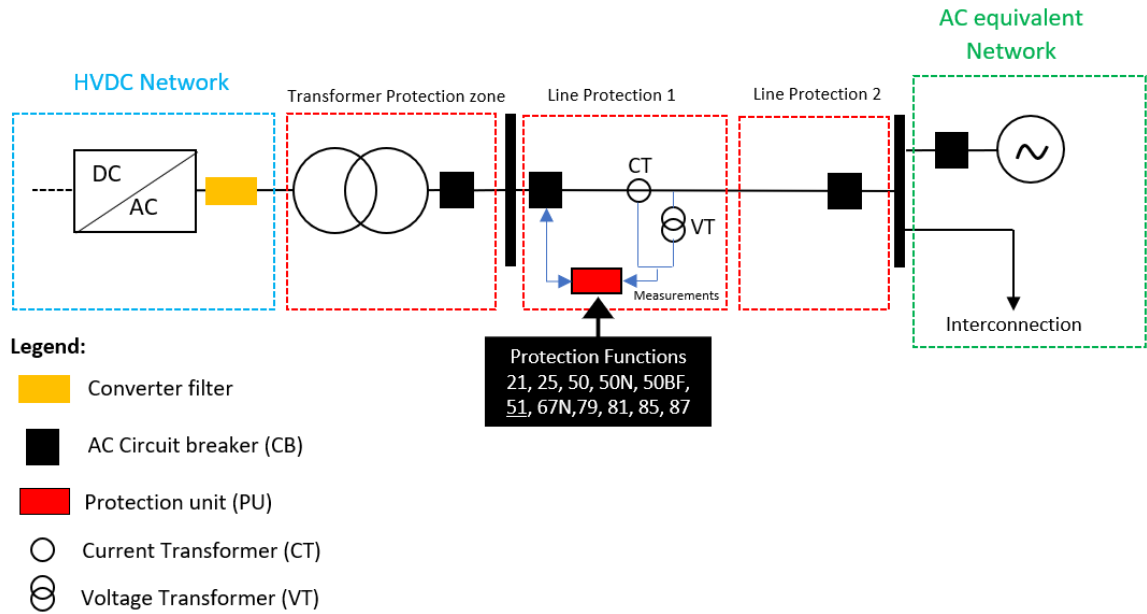


Figure 2: Test network model and Protection Functions

2.4 Conclusions

The application described in this section is a preliminary attempt to introduce a VSC converter in a tool used for Power system protection studies, to enable the study of the dynamic interaction interaction between the VSC and AC protection, with a focus on the protection performance.

Main outcomes:

- Understanding the model of the converter in CAPE and the possibility of performing dynamic studies with the tool, using CAPE-TS link;
- The main advantage of the this tool is the detail testing and modelling of the protection systems;
- At a first glance, the harmonic contribution from a converter is neglected with the current model, so this would require further investigation of CAPE capability and modelling;
- Definition of the test network and relevant protection functions to be modelled and run in CAPE for interaction studies.

Next steps:

- Integrate test network in CAPE;
- Perform initial steady state test for refining the relay parameters;
- Perform a dynamic study (study with PSSE);
- Assess the possibility to integrate additional tools with CAPE for dynamic interactions between converters and AC protections.

References

- [1] CAPE Official Website, <https://www.electrocon.com/capeintro.php>, Last accessed on the 16/01/2019.
- [2] Siemens acquires Electrocon, official press release, https://www.electrocon.com/news_18-01-Siemens.php, Last accessed on the 16/01/2019.
- [3] CAPE Client list, <https://www.electrocon.com/customers.php>, Last accessed on the 16/01/2019.
- [4] Short-Circuit and Relay coordination programs; <http://www.aspeninc.com/web/software/oneliner>, Last accessed on the 16/01/2019.
- [5] Dirk Van Hertem; Oriol Gomis-Bellmunt; Jun Liang, "HVDC Grids: For Offshore and Supergrid of the Future", IEEE, 2016
- [6] CAPE User Manual - Version 14, 2015, Electrocon International, Inc.
- [7] Working group, "Impact of Voltage Source Converter (VSC) Based HVDC Transmission on AC System Protection", IEEE, System Protection Subcommittee of the Power System Relaying and Control Committee, Technical Report, 2017.
- [8] "New Features in Short Circuit in the Computer-Aided Protection Engineering System (CAPE)", CAPE Users' Group, June 22-23, 2010, Michigan.

- [9] “Modelling Wind Generation for Fault Analysis in the Computer-Aided Protection Engineering System (CAPE)”, CAPE Users’ Group, Revised version from June 24-25 2008, February 17,2017, Michigan.
- [10] CAPE ST Link – PSSE integration, <https://www.electrocon.com/tslink.php>
- [11] PSSE software information, Link,Last accessed on the 16/01/2019.
- [12] IEEE Power and Energy Society, " C37.2-Standard Electrical Power System Device Function Numbers, Acronyms, and Contact Designations", Power Systems Relaying Committee, 3rd of October, 2008, New York.
- [13] General Electric, " ANSI Standard Device Numbers & Common Acronyms", Link , Last accessed 15/02/2019.
- [14] Source for image used in Figure 1, available at <https://www.midamericanenergy.com/>, Last accessed on the 16/01/2019.

3 DC protection studies using PSCAD software

Written by Wei Liu, approved by Jun Liang.

The section focuses on the interactions between system operations and dc fault protection within an HVDC transmission system. The studies are conducted in PSCAD/EMTDC software. To demonstrate the feasibility of the PSCAD/EMTDC to represent the problems, simulation results with PSCAD will be given in this section.

The section is organized as follows. The feasibility of PSCAD for the dc protection studies is illustrated first in Part 3.1. Introduction on the PSCAD/EMTDC software is given in Part 3.2. The modelling process of an HVDC grid in PSCAD/EMTDC is illustrated in Part 3.3. In Part 3.4, simulation results with PSCAD are shown demonstrating the interactions between VSCs and faults in a dc grid. Part 3.5 summarizes the work.

3.1 Feasibility of PSCAD for dc protection studies

A dc fault is a transient phenomenon on a hybrid AC/DC power system. Due to the high risks when a dc fault occurs in an HVDC system, many studies have been focusing on the analysis of dc faults both in time and frequency domain.

Time domain simulations, as powerful tools, are suitable to predict the consequence of a dc fault in an real HVDC system. The time-domain voltage and current waveforms within a system after a fault can give clear information on the fault consequence.

PSCAD (power systems CAD) as a graphical user interface of EMTDC (Electromagnetic Transients including DC), is most suitable for simulating the time domain instantaneous responses (also popularly known as electromagnetic transients) of electrical systems [1].

The following is a sample of the types of studies routinely conducted using EMTDC [2]:

- 1) Contingency studies of AC networks consisting of rotating machines, exciters, governors, turbines, transformers, transmission lines, cables, and loads
- 2) Relay coordination

- 3) Transformer saturation effects
- 4) Over-voltages due to a fault or breaker operation
- 5) Insulation coordination of transformers, breakers and arrestors
- 6) Control system design and coordination of FACTS and HVDC; including STATCOM, VSC, etc.
- 7) Optimal design of controller parameters

Based on the above functions, the studies of interactions between system operations and dc faults can be conducted in PSCAD/EMTDC.

3.2 Introduction of PSCAD/EMTDC software

EMTDC represents and solves differential equations (for both electromagnetic and electromechanical systems) in the time domain. Solutions are calculated based on a fixed time step, and its program structure allows for the representation of control systems, either with or without electromagnetic or electromechanical systems present.

EMTDC is a class of simulation tool, which differs from phasor domain solution engines, such as load-flow and transient stability programs. These tools utilize steady-state equations to represent electrical circuits, but will actually solve the differential equations of machine mechanical dynamics.

The power of EMTDC is greatly enhanced by its state-of-the-art graphical user interface called PSCAD. PSCAD allows the user to graphically assemble the circuit, run the simulation, analyze the results, and manage the data in a completely integrated graphical environment [2].

3.3 Modeling of an HVDC system in PSCAD/EMTDC

PSCAD is used extensively for many types of AC and DC power simulation studies. HVDC system operations, dc faults, and dc system protection can be implemented in PSCAD. Therefore PSCAD is selected as a tool to analyze the interactions between system operations and dc faults in HVDC systems.

An HVDC system normally contains of the main following parts:

- 1) AC systems and ac transmission lines to represent an ac power grid

- 2) AC Circuit Breakers (ACCBs) and its relays
- 3) Interface transformers between ac grids and converters
- 4) Converters (Inverters and Rectifiers)
- 5) DC transmission lines and reactors
- 6) DC Circuit Breakers (DCCBs) and its relays

The modeling of the each part in PSCAD/EMTDC will be given in this section to illustrate the whole system configurations and the dc protection process.

3.3.1 System modeling in PSCAD

- 1) AC system modelling

In the study of dc faults, ac systems in PSCAD are modelled as a ideal ac sources with specific SCRs (short circuit ratio) as shown in Figure 3. The impedance of the ac transmission lines is modelled as inductance and resistance. [3]

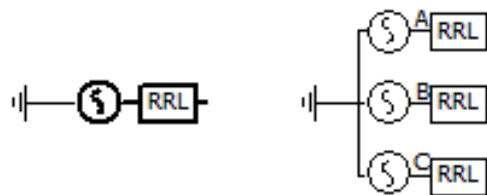


Figure 3: AC source with R/L circuits

- 2) Transformer modelling

The interface transformers are set as wye/delta or wye/wye transformers. Usually the grounding point is set on the grid side as shown in Figure 4. The saturation characteristic of the transformer can also be emulated by the unified magnetic equivalent circuit (UMEC) models [2], [4].

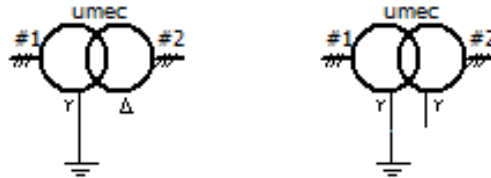


Figure 4: UMEC transformer models in PSCAD

3) Converter modelling

VSC based HVDC systems are employed in this section. Two-level VSC and MMC can be modelled in PSCAD/EMTDC. In order to show the converter dynamics during a dc fault, the models [5] as shown in Figure 5 are adopted in this study.

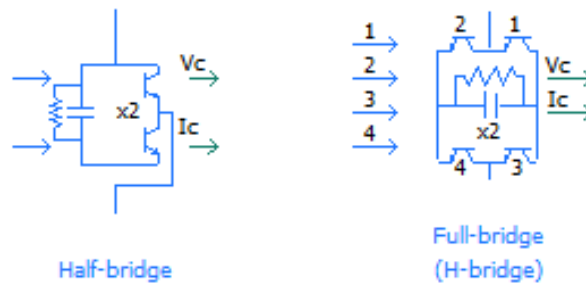


Figure 5: HB and FB MMC models in PSCAD

4) DC transmission line modelling

Both overhead lines (OHLs) and cables have been used in a HVDC system for a real project. The modelling of OHLs and cables can be implemented in PSCAD/EMTDC. Different modeling methods are proposed to model the transmission lines.

In PSCAD, there are different methods [6]-[8] to represent the transmission lines :

(1) PI-section model

This method uses lumped passive elements to emulate transmission lines, which is suitable to represent short transmission lines.

(2) Bergeron model

The Bergeron Model is based on single frequency model. The parameters are derived at a specified frequency. It is suitable to be used in the conditions where a specified frequency is most important.

(3) Frequency dependent model

Frequency dependent model can represent the frequency and distributed parameters in a wide frequency range. Thus, it is widely used in simulation studies. For dc fault studies, the frequency dependent model is employed.

3.3.2 Protection device modelling in PSCAD

1) AC circuit breaker (ACCB) modelling in PSCAD

An ACCB can be modelled as an ideal switch with a time delay. The zero-crossings of currents are necessary conditions for the ACCBs to switch off. An ACCB can be modelled as a ideal switch with a time delay (e.g. 2-3 cycles of AC components). It should be emphasized that the switch can only be switched off when there is a zero-crossing. The model of ACCBs in PSCAD is given in Figure 6

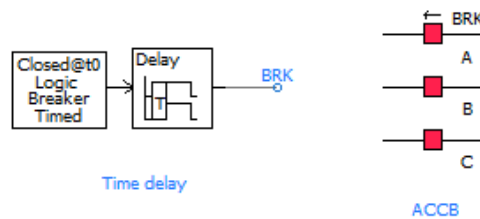


Figure 6: ACCB models in PSCAD

2) DC circuit breaker (DCCB) modelling in PSCAD

Hybrid DCCBs are used in this research to protect the VSC from a dc fault [10]. Normally, there are three branches in a hybrid DCCB, normal current path, current commutation path, and energy absorption path. The hybrid DCCB is modelled as an ideal switch with a paralleled arrester. The time delay is 2ms for a hybrid DCCB. The model built in PSCAD is given in Figure 7.

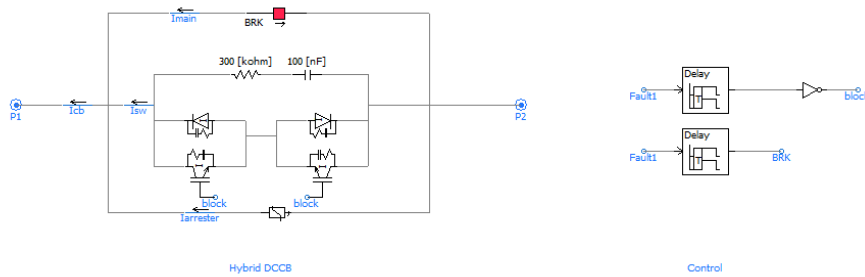


Figure 7: DCCB models in PSCAD

3.4 Simulation results on dc protection in PSCAD

- 1) DC fault with half-bridge MMCs
 - (A) Protecting dc fault with ACCBs

A dc fault can be isolated by switching off the ACCBs in the ac side of the VSC [9]. The time for the whole process is normally around 100ms. The VSC will be blocked immediately when a dc fault is detected. Before the ACCB is switched off, the VSC works as a uncontrollable rectifier. The ac side will still feed the fault current through the diodes (or thyristors) of the half-bridge submodules (HB-SMs). The ACCB will isolate the fault permanently, which normally takes approximately 100 ms. After the ACCB is switched off, the fault current will decay in the dc lines, which will also take hundreds of milliseconds. The waveforms are give in Figure 8.

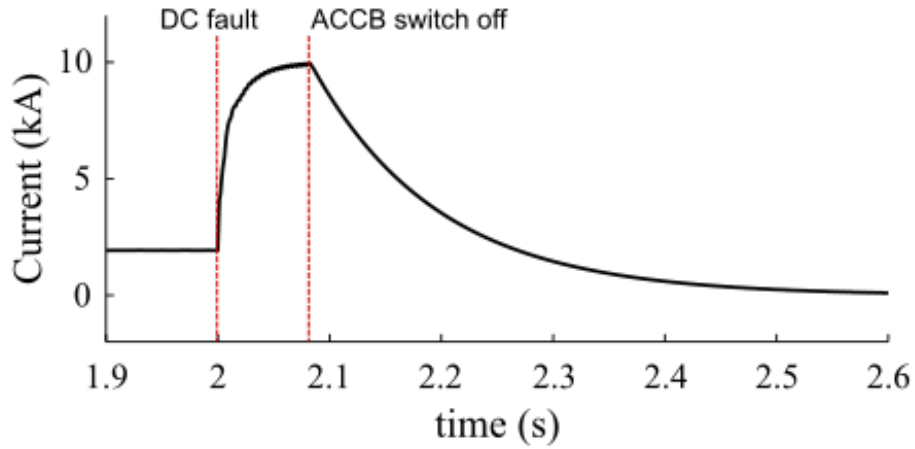


Figure 8: DC protection with ACCBs

(B) Protecting DC faults with DCCBs

The hybrid DCCBs can isolate a dc fault within several milliseconds, which is faster than that with ACCBs [11]. The waveforms are given in Figure 9. It can be seen that the dc fault is isolated within 6 ms with the hybrid DCCB.

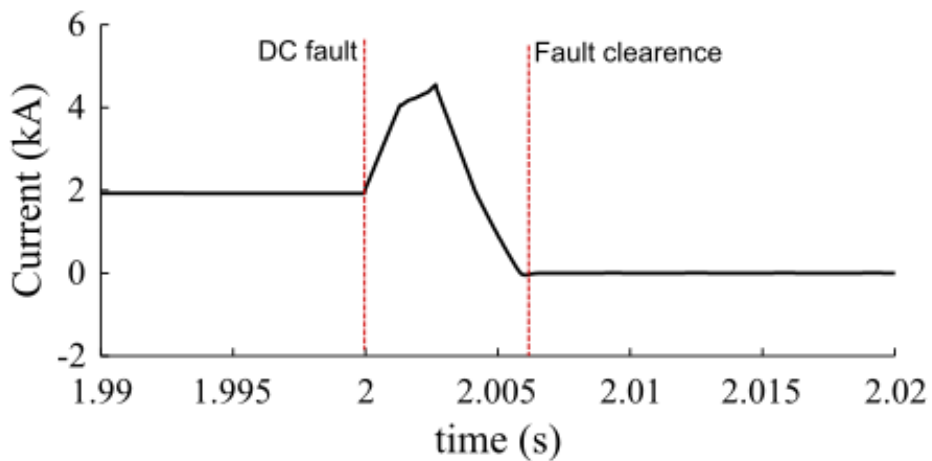


Figure 9: DC protection with DCCBs

2) Protecting dc faults with full-bridge MMCs

An MMC converter configured as a full-bridge can isolate a dc fault by itself [12]. When a dc side fault is detected by the FB-MMC, the FB-MMC can either be blocked or control its dc current to be zero. The advantage of the FB-MMC is that the converter itself can isolate the fault current through its control system. The waveforms are given in Figure 10.

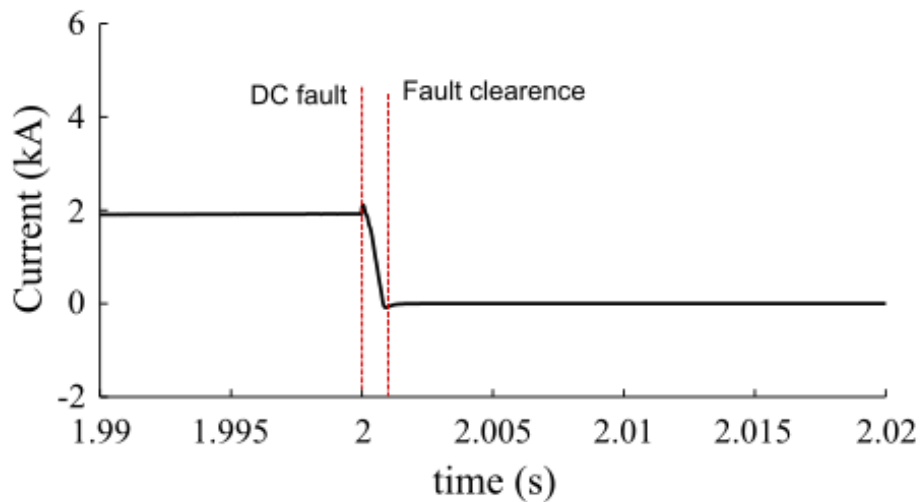


Figure 10: DC protection with DCCBs

It can be seen that with FB-MMCs, the dc fault current is reduced to zero more quickly than that with DCCBs or ACCBs. The maximum current provided by the converter is also much lower than the other two conditions.

3.5 Conclusion

This section are mainly focused on the interactions between converter operations and dc faults in an HVDC system. PSCAD/EMTDC is selected as a tool to carry on the research.

A hybrid AC/DC system can be built in PSCAD to study the transients of a dc fault in an HVDC system. Different dc protection technologies can also be implemented in PSCAD using suitable models.

The feasibility of the PSCAD software to represent the interactions between system operation and dc faults is verified by simulation results in PSCAD.

References

- [1] User'Guide: Transient Analysis for PSCAD Power System Simulation
- [2] PSCAD®/EMTDC™ vs 4.2 User'Guide, Manitoba HVDC Research Centre, 2005. <https://hvdc.ca/pscad/>
- [3] Jovcic D, Ahmed K. High-Voltage Direct Current Transmission: Converters Systems and DC Grids; Wiley: New York, 2015.
- [4] CHEN, M.S. AND DILLON, W.E. (1974), 'Power Systems Modeling', Proceedings IEEE, Vol. 62, No.7, July, pp. 901-915.
- [5] H. Saad, S. Dennezière, J. Mahseredjian, P. Delarue, X. Guillaud, J.Peralta, et al., "Modular multilevel converter models for electromagnetic transients," IEEE Transactions on Power Delivery, vol.29, no. 3, pp. 1481-1489, Jun. 2014.
- [6] PSCAD Online Help - Bergeron Line Model, v4.2.1 ed. Winnipeg, Canada: Manitoba HVDC Research Centre Inc., 2006
- [7] PSCAD Online Help - Model Selection, v4.2.1 ed. Winnipeg, Canada: Manitoba HVDC Research Centre Inc., 2006.
- [8] PSCAD Online Help - Frequency Dependent (Phase) Model, v4.2.1 ed. Winnipeg, Canada: Manitoba HVDC Research Centre Inc., 2006.
- [9] W. Leterme and D. Van Hertem, "Classification of Fault Clearing Strategies for HVDC Grids," in Proc. Cigré Lund Symp., Lund, Sweden, 27–28 May 2015.

- [10] J. Häfner and B. Jacobson, “Proactive Hybrid HVDC Breakers: A key innovation for reliable HVDC grids,” in CIGRÉ Bologna Symp., Bologna, Italy, 13- 15 Sep. 2011.
- [11] Cigre Joint Working Group A3-B4.34, “Technical Requirements and Specifications of State-of-the-art DC Switching Equipment,” Cigré Technical Brochure, 2017.
- [12] Zhang J, Zhao C. The research of SM topology with DC fault tolerance in MMC-HVDC. IEEE Transactions on PD. 2015; 30: 1561-1568.

4 Mutual Interactions and Stability Analysis of MMC-Based HVDC Link

Written by Saman Dadjo Tavakoli, approved by Eduardo Prieto and Oriol Gomis.

This section investigates the small-signal behavior and the mutual interactions of an HVDC link equipped with modular multi-level converters (MMC) at both ends. The nonlinear model of MMC with all control loops is derived and linearized to obtain a linear model suitable for small-signal analysis. The system eigenvalues and normalized participation factors are calculated in order to identify the critical modes of the system as well as the parameters of the system which highly contribute to instability. The analysis also reveals the interactions between the master and slave converters of the HVDC system.

The stability and interaction analysis are carried out using MATLAB software. The MATLAB-Simulink, along with the coding environment, is used to develop three models of the HVDC link: nonlinear time-domain model, linear time-domain model, and state-space frequency-domain model. The use of MATLAB software is due to its capability of conducting both time-domain and frequency-domain analysis.

4.1 Introduction

Modular multi-level converter (MMC) has emerged as the preferred choice for voltage source converter (VSC)-based HVDC systems mainly due to low losses, low harmonic distortion, scalability, and redundancy [1]. However, the control of MMC is more challenging than the control of the two-level VSC due to the extra control actions required for circulating current and submodule (SM) capacitor voltage unbalance compensation. The various control schemes proposed in the literature can be classified as follows. First, the non-energy-controlled method (also called uncompensated modulation) [2], including the direct voltage and the open-loop modulation [3]. These control methods are asymptotically stable but their transient responses depend on the MMC impedance rather than being dictated by the control systems, leading to slow and undesirable dynamics [4]. Moreover, they cause disturbances

that lead to circulating currents that should be eliminated using control techniques [5]. A second option is to implement an energy-controlled method, also known as compensated modulation or closed-loop modulation [2]. This control method does not generate parasitic voltage components, but energy controllers are required to ensure an asymptotically stable system [6].

In order to perform a small-signal analysis and to design the system controllers, a nonlinear model of the MMC-based HVDC link should be derived. In previous works, the linear model of a MMC is derived for system stability assessment [7], and the control system is designed based on the linear model [8]. This linearization can be further extended to include the entire model of MMC-based HVDC link. In [9], the linear state-space models of master MMC (controlling the dc link voltage), slave MMC (controlling ac power), and the HVDC cable are derived to analyze the system transient response, suggesting alternative controllers to improve the dynamic response. However, the present work analyzes the mutual interactions between control systems and the stability of a complete MMC-based HVDC link.

Considering an MMC-based HVDC link, the control systems of the master and slave MMCs would interact with each other through the HVDC cable. For instance, a change in the ac side of the slave MMC might cause a transient in the dc voltage control loop of master MMC. This section investigates the mutual interactions between control loops and the small-signal dynamics of an MMC-based HVDC link. First, the system configuration is explained and the control system of MMC is detailed. Then, the state-space equations of the complete system are derived and linearized. The linear models are connected together to build a MIMO model including all the system dynamics. The small-signal analysis is conducted on the MIMO model to identify critical modes through a participation factor and damping ratio analysis. Moreover, the sensitivity of the system to the critical parameters is studied and verified via time domain simulations. Finally, the interactions between various input/output pairs are investigated.

4.2 System Description

A typical HVDC link between two strong ac networks is shown in Figure 11. In such configuration, the master MMC regulates the dc voltage while the slave MMC controls the active power exchange [9]. Also, reactive power can be regulated at both ends. The averaged model of the MMC structure connected to an ac network is presented in Figure 12. The MMC consists of six

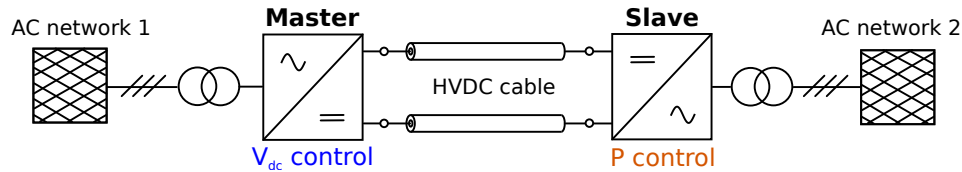


Figure 11: MMC-based HVDC link

arms, each of them contains N_{arm} half-bridge submodules with a capacitance C_{SM} and an arm reactor connected in series. The three legs, corresponding to three phases, can be divided in upper and lower arms. The six arms synthesize the required ac and dc voltages to achieve the desired power exchange between ac and dc sides.

The control system of the MMC is based on the energy-controlled approach and presented in Figure 13. The grid side current controller tracks the current references sent by the outer control loop. In case of master MMC, the dc voltage outer control loop provides the q-axis current reference, whereas in slave MMC, it is provided by the ac active power control loop. In both cases, the d-axis current reference is given by the reactive power control loop. In addition, the energy balancing and total energy control send the circulating current reference for the inner current controller. Furthermore, a Phase Locked Loop (PLL) tracks the ac voltage in the point of connection with the ac network. The outputs of the both current control systems (grid side and circulating) are used to generate the six arm voltages. Finally, the modulation and cells balancing algorithm are responsible for generating the required voltage through communication with the submodule switches.

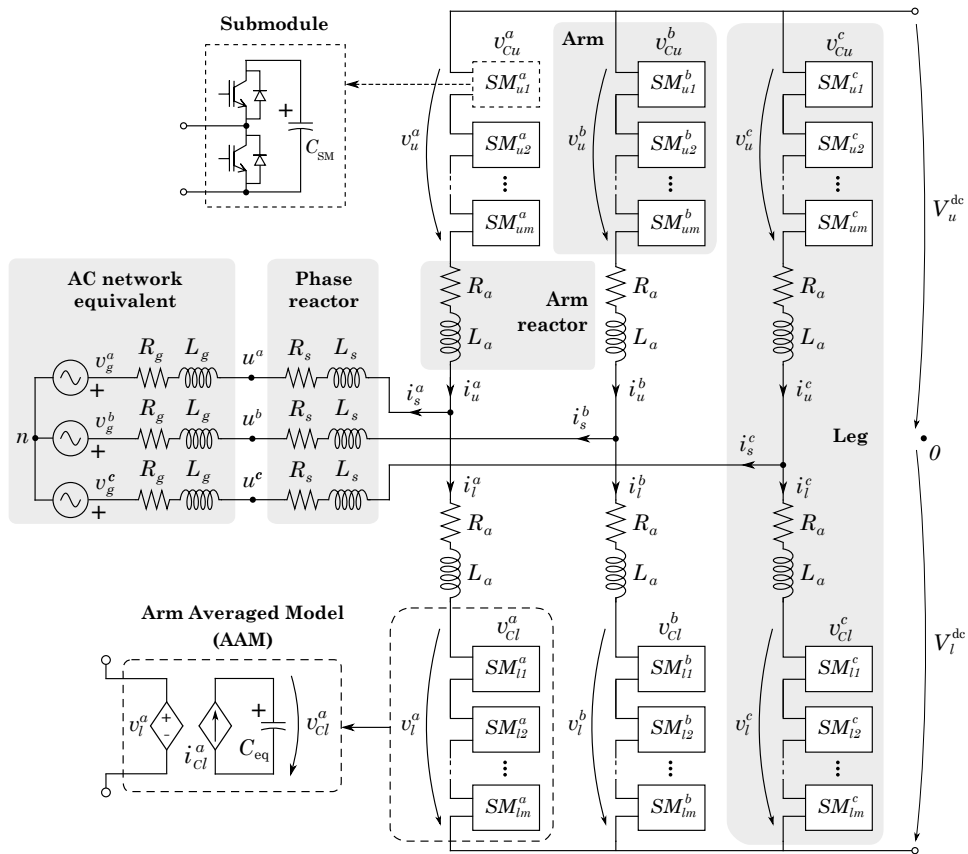


Figure 12: Averaged model of MMC connected to an ac network

4.3 System Modeling

4.3.1 Modular Multilevel Converter (MMC)

Referring to Figure 12, the electrical circuit equations per phase are

$$\begin{aligned}
 V_u^{\text{dc}} - v_u^j - v_g^j - v_n = \\
 R_a i_u^j + L_a \frac{di_u^j}{dt} + (R_s + R_g) i_s^j + (L_s + L_g) \frac{di_s^j}{dt}
 \end{aligned} \tag{1}$$

$$\begin{aligned}
 -V_l^{\text{dc}} + v_l^j - v_g^j - v_n = \\
 -R_a i_l^j - L_a \frac{di_l^j}{dt} + (R_s + R_g) i_s^j + (L_s + L_g) \frac{di_s^j}{dt}
 \end{aligned} \tag{2}$$

where, R_a and L_a are arm resistance and inductance; R_s and L_s are ac grid filter resistance and inductance; V_u^{DC} and V_l^{DC} are upper and lower voltages of the HVDC link. The ac grid current and Thévenin voltage are, respectively, i_s^j and v_g^j , while the voltages applied by the upper and lower arms are v_u^j and v_l^j . The currents flowing through the upper and lower arms are indicated by i_u^j and i_l^j , respectively.

The following variable change is common in MMC modeling

$$\left\{ \begin{array}{l} v_{\text{diff}}^j \triangleq \frac{1}{2}(-v_u^j + v_l^j) \\ v_{\text{sum}}^j \triangleq v_u^j + v_l^j \\ i_{\text{sum}}^j \triangleq \frac{1}{2}(i_u^j + i_l^j) \\ R \triangleq R_s + R_g + \frac{R_a}{2} \\ L \triangleq L_s + L_g + \frac{L_a}{2} \end{array} \right. \quad \left\{ \begin{array}{l} v_u^j = -v_{\text{diff}}^j + \frac{1}{2}v_{\text{sum}}^j \\ v_l^j = v_{\text{diff}}^j + \frac{1}{2}v_{\text{sum}}^j \\ i_u^j = \frac{1}{2}i_s^j + i_{\text{sum}}^j \\ i_l^j = -\frac{1}{2}i_s^j + i_{\text{sum}}^j \end{array} \right. \tag{3}$$

where, v_{diff}^j is the differential voltage, approximately equal to the ac voltage at the point of connection. i_{sum}^j is the additive current circulating from the upper to the lower arm of the leg j ($j = a, b, c$). The additive voltage is indicated by v_{sum}^j and it is approximately equal to the sum of the dc poles voltages.

Adding and subtracting (1) and (2) and using the variable change given

by (3) would lead to

$$\frac{1}{2}(V_u^{\text{dc}} - V_l^{\text{dc}}) + v_{\text{diff}}^j - v_g^j - v_n = R i_s^j + L \frac{d i_s^j}{dt} \quad (4)$$

$$v_{\text{sum}}^j - (V_u^{\text{dc}} + V_l^{\text{dc}}) = -2R_a i_{\text{sum}}^j - 2L_a \frac{d i_{\text{sum}}^j}{dt} \quad (5)$$

The equations (4) and (5) are decoupled and only contain a single derivative term (i_s^j and i_{sum}^j); hence, they are suitable for state-space representation. The current i_{sum}^j contain ac and dc terms which impact the performance of the control system in various aspects. The dc term of i_{sum} can be transformed into $(\alpha\beta 0)$ frame. The zero component is used for the control of the power flow into the dc grid, while the $(\alpha\beta)$ components regulate the internal power exchange between legs. The ac term of i_{sum} contains $(+ - 0)$ sequences. The zero sequence is controlled to zero avoiding ac distortion in the dc grid, whereas $(+ -)$ sequences can be used to regulate the internal power exchange between upper and lower arms of each leg. A comprehensive discussion can be found in [4].

Since i_{sum} contains ac term with various frequencies, the transformation into (dq) frame becomes complicated. However, these components are relevant for the dc pole imbalance studies [10]. Considering only the dc term of i_{sum} , the system becomes suitable for linearization. Using the following definitions

$$V_{\text{off}}^{\text{dc}} \triangleq \frac{1}{2}(V_u^{\text{dc}} - V_l^{\text{dc}}), \quad V_t^{\text{dc}} \triangleq V_u^{\text{dc}} + V_l^{\text{dc}} \quad (6)$$

combined with (4) and (5), yields

$$v_{\text{diff}}^{\text{abc}} - v_g^{\text{abc}} + (V_{\text{OFF}}^{\text{dc}} - v_n)(1 \ 1 \ 1)^T = R \mathcal{I}_3 i_s^{\text{abc}} + L \mathcal{I}_3 \frac{d i_s^{\text{abc}}}{dt} \quad (7)$$

$$v_{\text{sum}}^{\alpha\beta 0 \text{dc}} - V_t^{\text{dc}}(0 \ 0 \ 1)^T = -2R_a \mathcal{I}_3 i_{\text{sum}}^{\alpha\beta 0 \text{dc}} - 2L_a \mathcal{I}_3 \frac{d i_{\text{sum}}^{\alpha\beta 0 \text{dc}}}{dt} \quad (8)$$

where \mathcal{I}_n is an identity matrix of order n .

4.3.2 MMC Control

The detailed control system of master/slave MMC is presented in Figure 13. The control system has the two main parts detailed above, the grid control and the energy control parts. This control system is used in the nonlinear

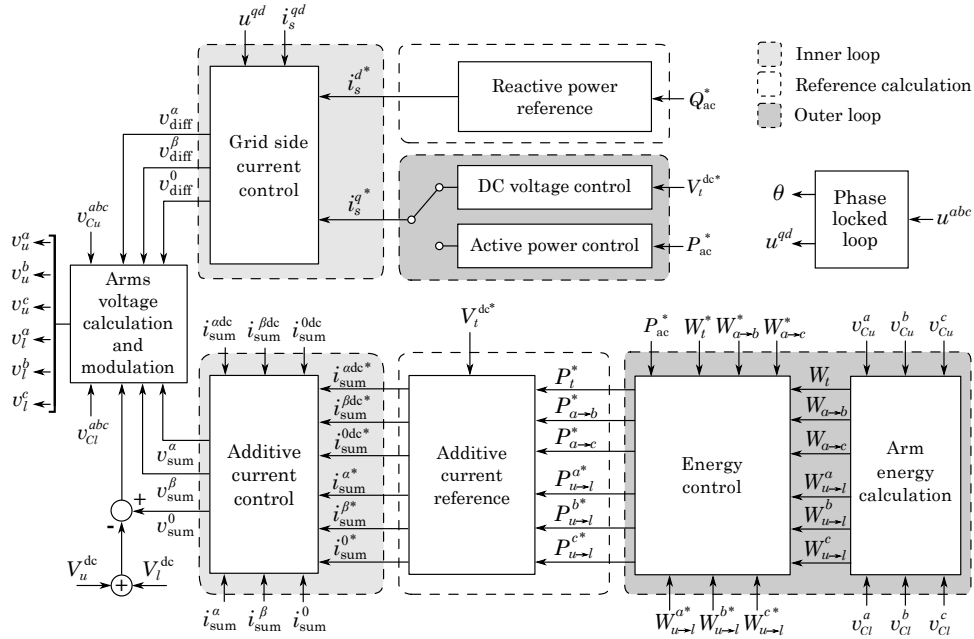


Figure 13: MMC energy-based control system

model of MMCs. However, for the small-signal analysis, it is assumed that the internal energy balance is properly performed; so only a total energy control is required to regulate the zero component of i_{sum} [11]. Based on this assumption, the linear model derivation can be simplified while maintaining a high level of accuracy. The control system with total energy control is presented in Figure 14. The outer control loop regulates total energy of the MMC (W_t) and generates the reference for the inner additive current (i_{sum}^{0dc*}) control loop.

4.3.3 HVDC Cable

The HVDC cable is modeled using a lumped parameters vector fitting method introduced in [12]. In the present case, a five-section model is considered to account for the hyperbolic correction factors, which makes the model more accurate specifically for long cables.

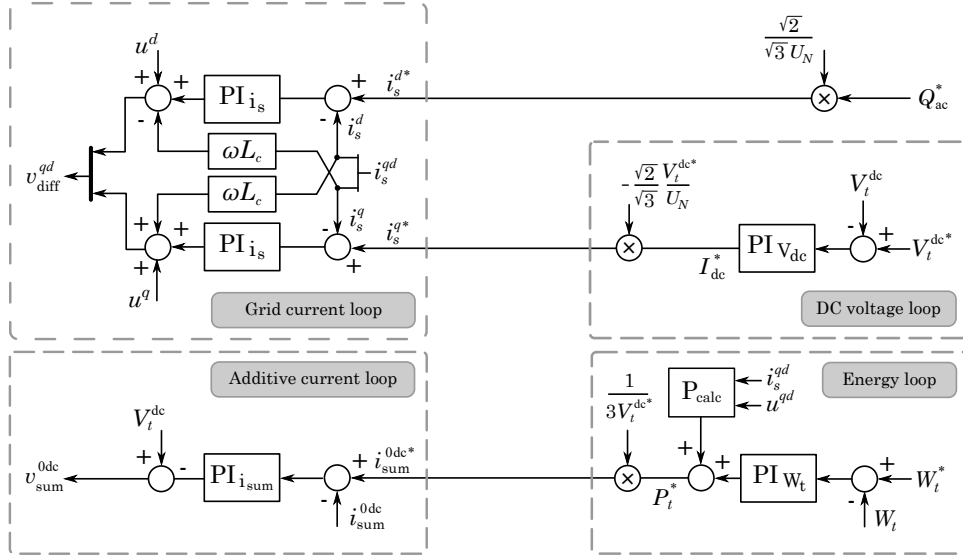


Figure 14: The control system of the master MMC in linear model

4.4 System Linearization

The small signal models of the master and slave MMCs, its corresponding controllers and the HVDC cable are derived and interconnected together to build a MIMO model which is able to represent the complete system dynamics. The model has 43 state variables, 4 outputs, and 10 inputs. The inputs/outputs are selected combining control and physical variables. The state-space representation of the HVDC link is given by

$$\Delta \dot{x} = \mathbf{A} \Delta x + \mathbf{B} \Delta u, \quad \Delta y = \mathbf{C} \Delta x + \mathbf{D} \Delta u \quad (9)$$

where Δx is a state vector including 43 states of the entire HVDC link, Δu is the input vector containing 10 desired inputs, and Δy is the output vector which includes 4 closed-loop control outputs. The master MMC has two main closed-loop cascaded control systems which are dc voltage control V_t^{dc} and total energy control W_t . In case of slave MMC, it has an active power control loop P_{n2} and again a total energy control. For the sake of clarity, the master MMC is indicated as MMC 1 and the slave as MMC 2 in the equations, then the input and output vectors can be defined as

$$\begin{aligned} \Delta u &= (\Delta V_t^{dc*}, \Delta P_2^*, \Delta W_{t1}^*, \Delta W_{t2}^*, \Delta v_{g1}^{qd}, \Delta v_{g2}^{qd}, \Delta Q_1^*, \Delta Q_2^*) \\ \Delta y &= (\Delta v_t^{dc}, \Delta p_2, \Delta w_{t1}, \Delta w_{t2}) \end{aligned} \quad (10)$$

4.4.1 MMC Linearization

Combining (7) and (8), three linear state-space equations can be derived. The three state variables are Δi_s^q , Δi_s^d , and Δi_{sum}^0 . In addition, there is one more state-space equation related to the total energy of MMC

$$\begin{aligned} \frac{dW_t}{dt} = & -\frac{3}{2}I_s^q \Delta v_{diff}^q - \frac{3}{2}I_s^d \Delta v_{diff}^d - \frac{3}{2}V_{diff}^q \Delta i_s^q \\ & -\frac{3}{2}V_{diff}^d \Delta i_s^d + 3I_{sum}^{0dc} \Delta v_{sum}^{0dc} + 3V_{sum}^{0dc} \Delta i_{sum}^{0dc} \end{aligned} \quad (11)$$

where I_s^q , I_s^d , V_{diff}^q , V_{diff}^d , I_{sum}^{0dc} , and V_{sum}^{0dc} are constant values at the operating point.

4.4.2 Control System Linearization

The linearization of the PLL and ac active power equation (for MMC 2) are required. The PLL regulates u^d to zero with a PI controller. The angle deviation introduced by PLL can have an impact on the dynamics of the closed loop control system. It can be linearized as

$$\Delta e_\theta = -\frac{k_{p-pll}s + k_{i-pll}}{s^2 + u_0^q k_{p-pll}s + u_0^q k_{i-pll}} \Delta u^d \quad (12)$$

This angle deviation is used for transformation from converter qd frame (x^{qdc}), used by the control loops, and the grid qd frame (x^{qd}) used to represent the real values [12]. Moreover, the active power equation is linearized as

$$\Delta P = \frac{3}{2}(U^q \Delta i_s^q + \Delta u^q I_s^q + U^d \Delta i_s^d + \Delta u^d I_s^d) \quad (13)$$

4.4.3 Complete Linear Model

The complete linear model of the HVDC link is shown in Figure 15. Earlier, in the linear model, the total energy of the converter is controlled using a cascaded current loop, assuming that the energy balance between the legs and upper and lower arms is performed in an adequate manner. The validation of the linear model is performed through a time domain simulation, in which a detailed nonlinear model of the MMC with the complete control system shown in Figure 13 is used. A 10% step change in the active power (ΔP_2) is applied to the nonlinear and linear models. The responses related to various

variables in MMC 1 are shown in Figure 16, which confirms the accuracy of the linear model. The parameters of the system can be found in Table I and II of the appendix.

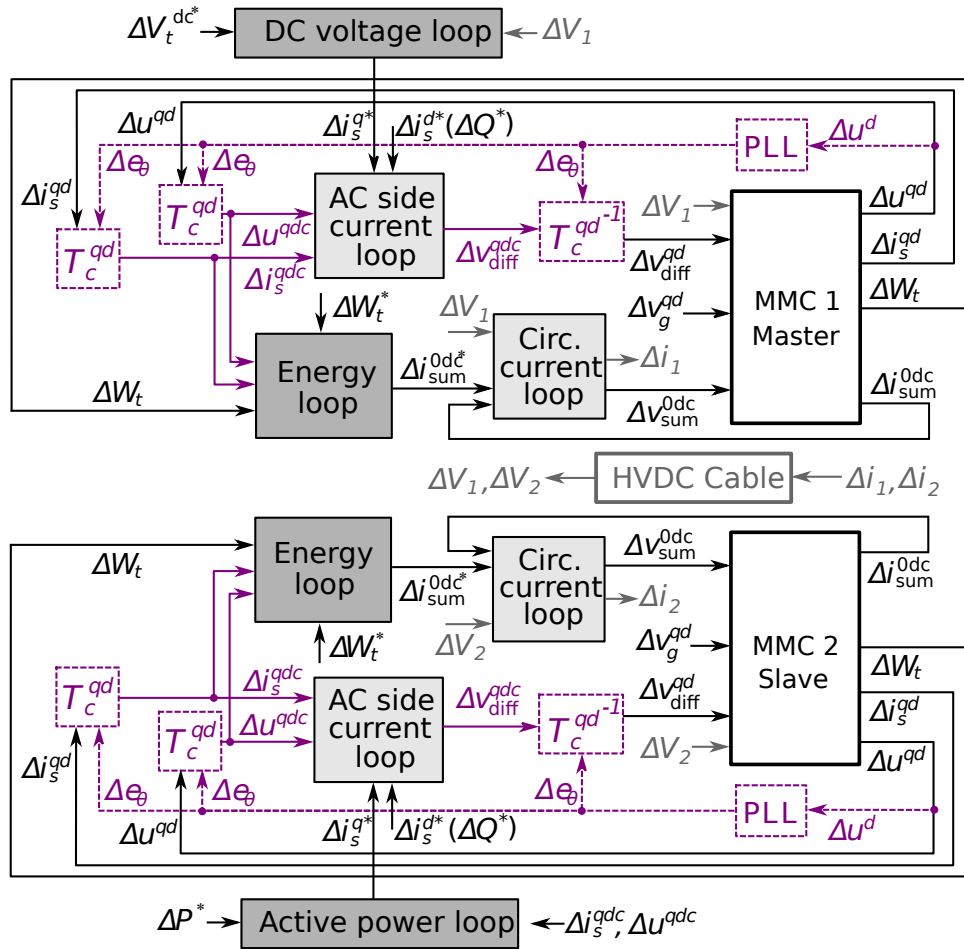


Figure 15: Linear model of the HVDC link with cascaded total energy control loop

The MIMO model presented in Figure 17 is built from the linear model. The complete state-space model is transformed into Laplace domain and the system transfer function matrix, $T_{sys}(s)$, relating the different input-output variables, including the corresponding control loops, is derived.

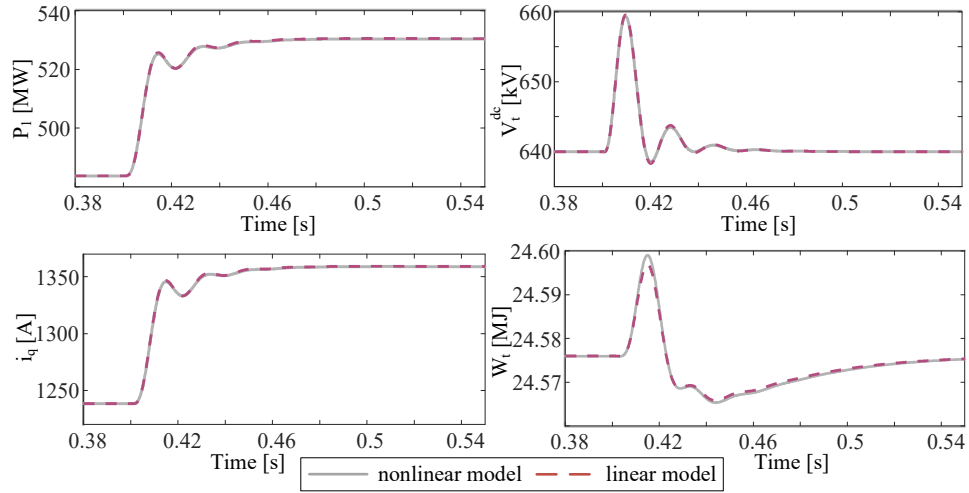


Figure 16: Validation of the linear model against nonlinear model (MMC 1)

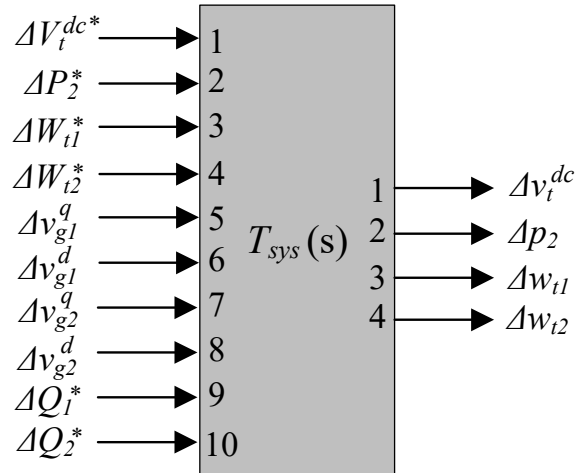


Figure 17: MIMO presentation of the linear model of the HVDC link

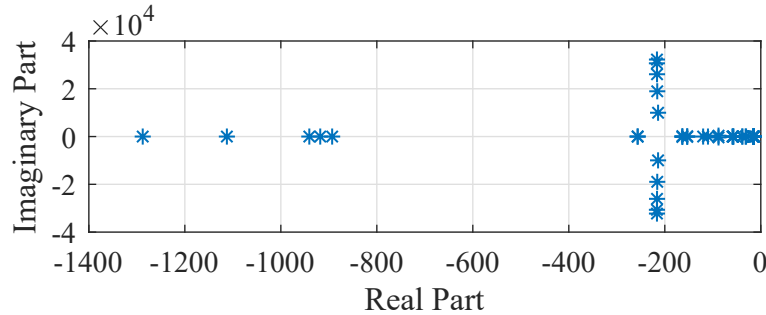


Figure 18: Eigenvalues of the HVDC link

4.5 System Analysis

Once the transfer matrix $T_{sys}(s)$ is obtained, the small-signal analysis can be conducted. In the following sections, the system eigenvalues, sensitivity, and mutual interactions are studied.

4.5.1 Eigenvalue Analysis

The eigenvalue analysis is conducted on the linear model of the HVDC link. The system has 43 state variables and therefore 43 eigenvalues, of which 11 states belong to MMC 1, 11 states MMC 2, and 21 states are related to cable model. Assuming the cable length is 50 km, the eigenvalues of the system are shown in Figure 18. In order to find critical modes, the damping ratio (D) is defined for every eigenvalue (λ_i) as $D = -\text{Re}(\lambda_i)/\text{abs}(\lambda_i)$.

Among 43 system eigenvalues, 10 of them have a very low damping ratio (lower than 5%). Next, there are 2 eigenvalues with moderately low damping ratio, which is around 23%. The rest of the eigenvalues are highly damped. Hence, these 12 eigenvalues are considered to be the critical modes of the system. It is also noted that 10 of the critical modes have a high frequency (HF) with the order of 10^4 rad/s, whereas 2 of them have a relatively low frequency (LF) of 375.8 rad/s. We will refer to them as HF and LF critical modes, respectively.

In order to find the parameters of the system which contribute to the 12 critical modes, a normalized participation factor (nPF) analysis is conducted. The nPF, damping ratio, state variable index, and eigenvalue index are presented in Figure 19. Eigenvalue indexes 1 to 10 are assigned to HF modes, while indexes 14 and 15 are related to LF modes. The rest of the eigenvalue

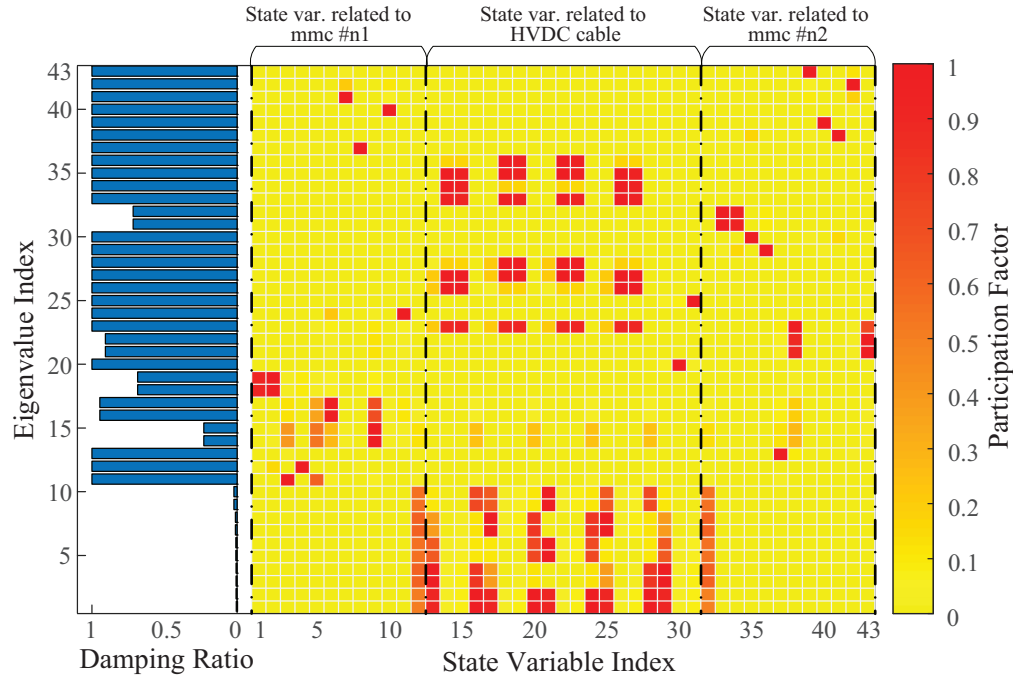


Figure 19: Normalized participation factor and damping ratio of the system

indexes contribute very little to the critical modes. It is also noted that the PI controller of the dc voltage control loop (MMC 1) highly contribute to the LF modes (eigenvalue indexes 14 and 15 with $nPF=1$).

Therefore, it can be concluded that two components of the HVDC link are likely to cause instability; first, the parameters of the HVDC cable, and second, the PI controller of the dc voltage control loop.

4.5.2 Sensitivity Analysis

Since the the parameters of the HVDC cable and the PI controller of the dc voltage control loop mainly contribute to the HF and LF critical modes, the sensitivity of the system against the variations of cable length and the coefficients of the PI controller is investigated.

The cable length is changed from 250 km to only 5 km. As it is presented in Figure 20, the eigenvalues move towards the right half plane, reducing system stability margin. The transient response of the dc voltage and total energy control loops of MMC 1 are shown in Figure 21. The ac power injected

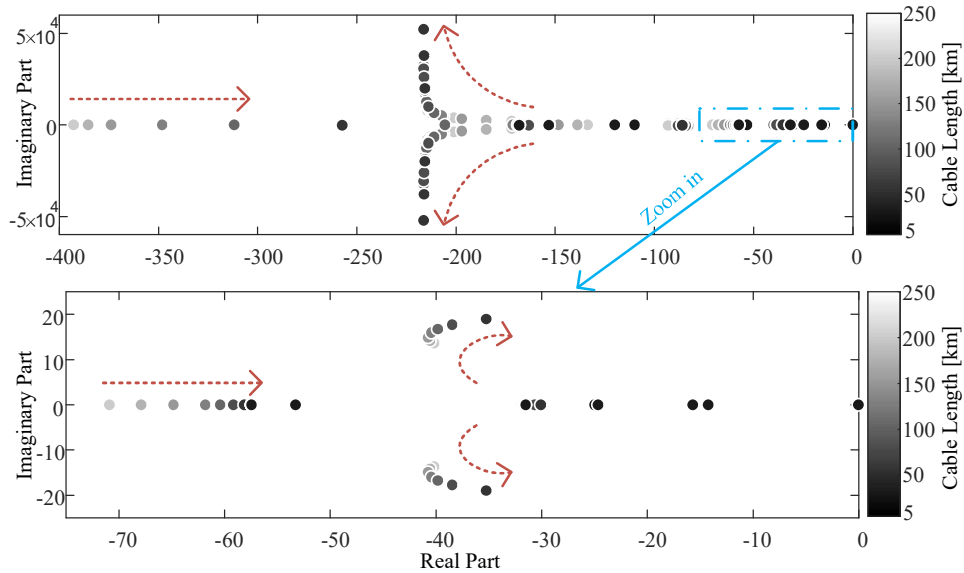


Figure 20: (Dominant) Eigenvalues for various cable lengths. The top plot is magnified in the bottom plot

into the ac grid by MMC 2 is increased by 20% at $t=0.4$ s and then reduced again by the same amount at $t=0.65$ s. It is observed that for the shorter cable length, the system exhibits higher oscillations (lower damping), which is consistent with the eigenvalue analysis.

To investigate the sensitivity of the system against the PI controller of dc voltage, the cable length is set to 50 km and the gain of the PI controller (both of integral and proportional gains), G , is reduced from 1 to 0.4. The dominant eigenvalues of the system are shown in Figure 22. By reducing G , the stability of the system is reduced as well, leading to instability for the values of G lower than 0.4. This is also indicated in the transient response of the nonlinear model which is presented in Figure 23. The dc voltage and total energy controllers of MMC 1 become oscillatory for smaller values of G .

4.5.3 Mutual Interactions

Referring to Figure 17, the MIMO model of the system provides information about the mutual interactions between all control loops related to MMC 1 and MMC 2. For instance, we can quantify the interactions between the

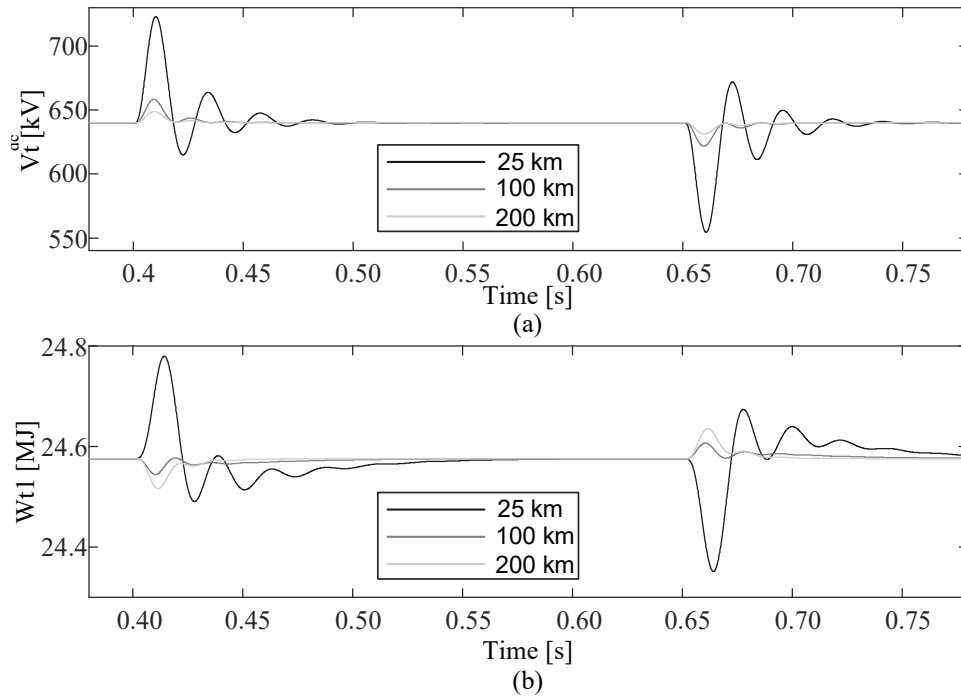


Figure 21: The transient response of (a) dc voltage and (b) the total energy control loops of MMC 1 for three different cable lengths

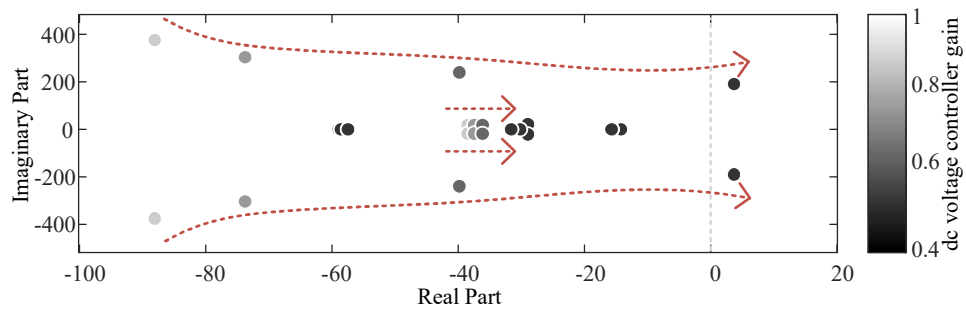


Figure 22: (Dominant) Eigenvalues for various dc voltage controller gains G

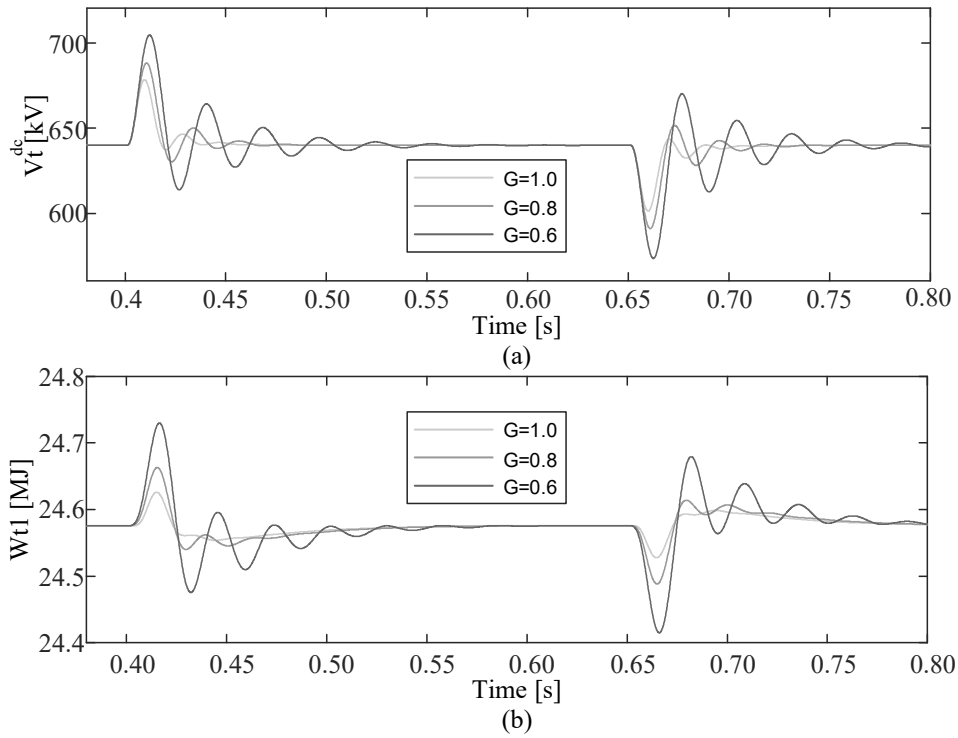


Figure 23: Transient response of (a) dc voltage and (b) the total energy control loops of MMC 1 for various gains of dc voltage controller (G)

total energy control loops of both MMCs.. In fact, with the MIMO model, we have the pole/zero map for any desired input/output pairs. Therefore, the performance of the control loops can be studied for any desired input. The responses of v_t^{dc} for step changes in the energy references, W_{t1}^* , W_{t2}^* , and q-axis grid voltages on the both sides of the HVDC link, v_{g1}^q , v_{g2}^q , are presented in Figure 24 (a). It is noted that the dc voltage control loop of MMC 1 is more vulnerable to the dynamics of the ac grid on the ac side of MMC 2. This might be due to the fact that the HVDC cable is a medium to transfer this dynamic variations to the dc voltage control loop, and therefore the critical modes of the cable might be excited. The impact of energy reference changes of both MMC 1 and 2 is insignificant.

Furthermore, unlike the sensitivity of the dc voltage control loop to the variations of v_{g2}^q , the total energy control of MMC 1 is sensitive to the variations of v_{g1}^q , as shown in Figure 24 (b). As a result, the dc voltage control loop of MMC 1 should be designed while considering the dynamics of the ac side of MMC 2, whereas the total energy control loop of MMC 1 should take account of the dynamics of the ac side of MMC 1.

4.6 Conclusion

In this section, the small-signal stability and mutual interactions of a MMC-based HVDC link have been investigated. The nonlinear system was linearized and the eigenvalues and participation factor have been calculated. It is noted that the critical modes of the system are related to the cable parameters and the PI controller of the dc voltage control loop of master MMC. The stability margin of the HVDC link reduces for the shorter cable length (below 10 km). Moreover, it is identified that the dc voltage control loop of master MMC significantly interacts with the ac side of slave MMC, while total energy control loop of master MMC is more influenced by the ac side of slave MMC.

4.7 Appendix

The following Clarke (15) and Park (16) transformations have been used. Note that regarding Park transformation, the electrical machinery notation

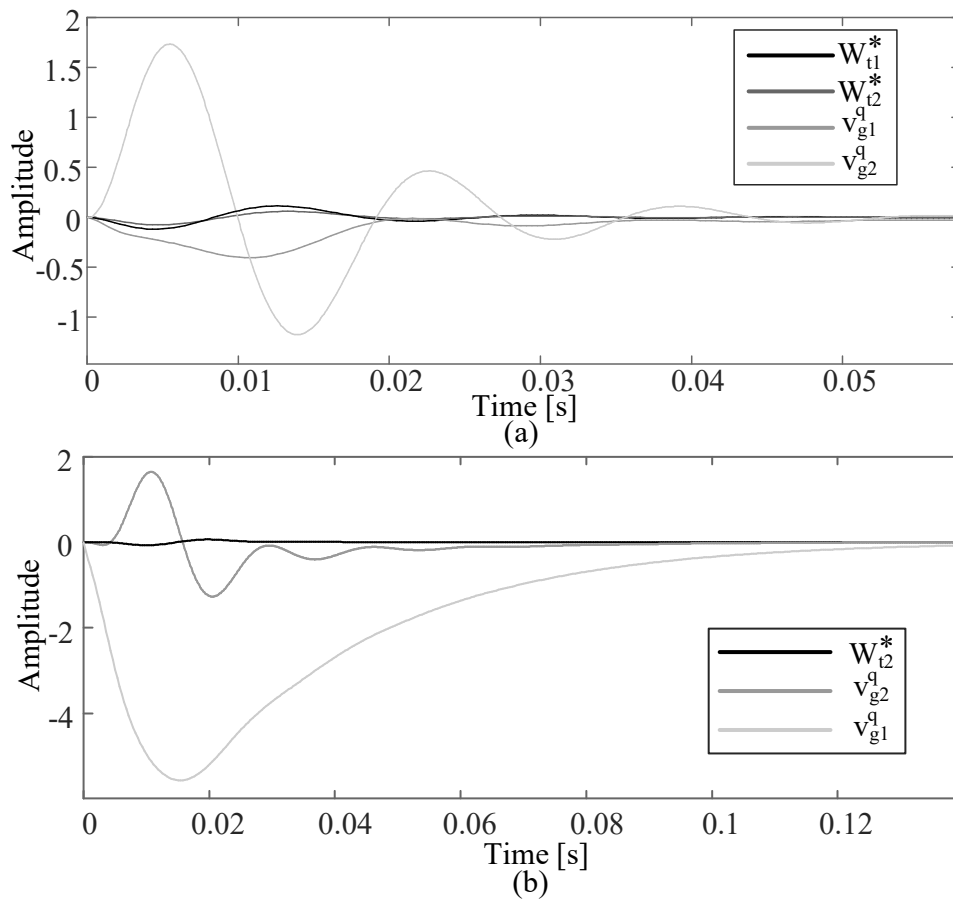


Figure 24: Step response of (a) the dc voltage control and (b) the total energy control of MMC 1 (w_{t1}) for various inputs

Table 2: MMC and AC grid parameters

Parameter	Symbol	Value	Units
Rated (base) active power	P_N	500	MW
Rated (base) ac-side voltage	U_N	320	kV rms ph-ph
Rated (base) dc-side voltage	V_{dc}	± 320	kV
Grid short-circuit ratio	SCR	10	-
Coupling impedance	$R_s + jL_s$	0.01+j0.2	pu
Arm reactor impedance	$R_a + jL_a$	0.01+j0.2	pu
Converter modules per arm	N_{arm}	400	-
Average module voltage	V_{SM}	1.6	kV
Sub-module capacitance	C_{SM}	8	mF

Table 3: HVDC cable parameters

Symbol	Value	Units	Symbol	Value	Units
r_1	0.1265	Ω/km	l_1	0.2644	mH/km
r_2	0.1504	Ω/km	l_2	7.2865	mH/km
r_3	0.0178	Ω/km	l_3	3.6198	mH/km
c	0.1616	$\mu\text{F}/\text{km}$	g	0.1015	$\mu\text{S}/\text{km}$

(qd0) is used

$$\Theta^{\alpha\beta 0} = \frac{1}{3} \begin{bmatrix} 2 & -1 & -1 \\ 0 & -\sqrt{3} & \sqrt{3} \\ 1 & 1 & 1 \end{bmatrix} \Theta^{abc} \quad (15)$$

$$\Theta^{qd0} = \frac{2}{3} \begin{bmatrix} \cos(\theta) & \cos\left(\theta - \frac{2\pi}{3}\right) & \cos\left(\theta + \frac{2\pi}{3}\right) \\ \sin(\theta) & \sin\left(\theta - \frac{2\pi}{3}\right) & \sin\left(\theta + \frac{2\pi}{3}\right) \\ \frac{1}{2} & \frac{1}{2} & \frac{1}{2} \end{bmatrix} \Theta^{abc} \quad (16)$$

The parameters of the MMCs and ac grids are given in Table I, while the HVDC cable parameters are provided in Table II.

References

- [1] J. Khazaei, M. Beza and M. Bongiorno, "Impedance Analysis of Modular Multi-Level Converters Connected to Weak AC Grids," in *IEEE Transactions on Power Systems*, vol. 33, no. 4, pp. 4015-4025, July 2018.
- [2] G. Bergna, J. A. Suul, S. D'Arco, "State-space modelling of modular multilevel converters for constant variables in steady-state", *Proc. IEEE 17th Workshop Control Modeling Power Electron. (COMPEL)*, pp. 1-9, Jun. 2016.
- [3] L. Harnefors, A. Antonopoulos, S. Norrga, L. Ängquist, H.-P. Nee, "Dynamic analysis of modular multilevel converters", *IEEE Trans. Ind. Electron.*, vol. 60, no. 7, pp. 2526-2537, Jul. 2013.
- [4] E. Prieto-Araujo, A. Junyent-Ferré, C. Collados-Rodríguez, G. Clariana-Colet, O. Gomis-Bellmunt, "Control design of modular multilevel converters in normal and AC fault conditions for HVDC grids", *Electr. Power Syst. Res.*, vol. 152, pp. 424-437, Nov. 2017.
- [5] Q. Tu, Z. Xu, L. Xu, "Reduced switching-frequency modulation and circulating current suppression for modular multilevel converters", *IEEE Trans. Power Del.*, vol. 26, no. 3, pp. 2009-2017, Jul. 2011.
- [6] K. Sharifabadi, L. Harnefors, H. P. Nee, S. Norrga, R. Teodorescu, *Design Control and Application of Modular Multilevel Converters for HVDC Transmission Systems*, Hoboken, NJ, USA:Wiley, 2016.
- [7] A. Jamshidifar, D. Jovcic, "Small-signal dynamic DQ model of modular multilevel converter for system studies", *IEEE Trans. Power Del.*, vol. 31, no. 1, pp. 191-199, Feb. 2016.
- [8] E. Sánchez-Sánchez, E. Prieto-Araujo, O. Gomis-Bellmunt, "Multi-terminal HVDC voltage droop control design considering DC Grid AC Grid and MMC dynamics", *Proc. 13th IET Int. Conf. AC DC Power Transmiss.*, pp. 1-6, 2017.
- [9] E. Sánchez-Sánchez, E. Prieto-Araujo, A. Junyent-Ferré and O. Gomis-Bellmunt, "Analysis of MMC Energy-Based Control Structures for VSC-HVDC Links," in *IEEE Journal of Emerging and Selected Topics in Power Electronics*, vol. 6, no. 3, pp. 1065-1076, 2018.

- [10] A. Junyent-Ferré, P. Clemow, M. M. C. Merlin, T. C. Green, "Operation of HVDC modular multilevel converters under DC pole imbalances", Proc. 16th Eur. Conf. Power Electron. Appl. (EPE-ECCE), pp. 1-10, Aug. 2014.
- [11] G. Bergna, J. A. Suul and S. D'Arco, "Impact on small-signal dynamics of using circulating currents instead of AC-currents to control the DC voltage in MMC HVDC terminals," 2016 IEEE Energy Conversion (ECCE), Milwaukee, WI, 2016, pp. 1-8.
- [12] J. Beerten, S. D'Arco, J. A. Suul, "Frequency-dependent cable modelling for small-signal stability analysis of VSC-HVDC systems", IET Generat. Transmiss. Distrib., vol. 10, no. 6, pp. 1370-1381, 2016.

5 AC transient stability interactions

Written by Nathalia de Moraes Dias Campos, approved by Jef Beerten.

Power systems are continuously subject to disturbances from which they must be able to recover in order to guarantee continuity of energy supply. This is a task that becomes increasingly difficult with the growing number of power-electronic devices in the grid as a result of the use of HVDC, renewable energy and FACTS devices. The increased complexity of power systems gives rise to new forms of interactions between components that had not been observed before and that pose a risk to system stability.

Over the years, several software tools have been developed to help engineers perform power systems studies in order to evaluate, among many other aspects, whether there are any stability risks. However, in the past there was a much clearer distinction of what software tools should be used for which system studies. This distinction has been blurred with the introduction of power-electronic devices in the grid and has created a need to reassess to which extent and in which cases the tools remain valid.

In this chapter, the main focus is on converter interactions at frequencies in the slower oscillation spectrum reaching up to a few tens of Hertz as highlighted in Figure 25. It intends to provide a brief comparison between two of the main types of software tools used to study interactions in this frequency range: electromagnetic transients and transient stability programs.

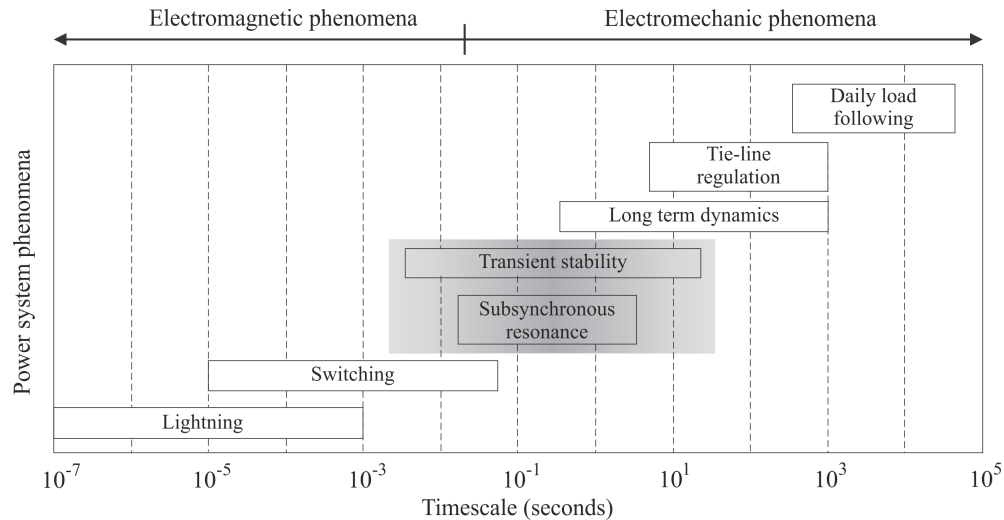


Figure 25: Timescale for power system phenomena.

At first, a brief overview of both type of programs is provided. This is followed by a review of the models generally recommended for representing the main power system components. Finally, a representative commercial software is chosen for each class of simulation tools and we examine which models are available for practical use in the two programs chosen.

5.1 Available software routines

As mentioned previously, there are two main classes of programs that are used for stability studies within the slower frequency range mentioned in the previous section. These are the electromagnetic transient (EMT)-type programs and electromechanical simulation programs (also known historically as transient stability programs or RMS-based programs).

In EMT-type programs, all components of the power system, including the network, are modelled through a set of differential equations which are solved in order to find the variables' instantaneous values. Assuming the proper models are used, it is possible to obtain an accurate response over a wide frequency range.

In electromechanical simulations the system variables are represented in their quasi steady-state phasor form (also called RMS form). It is assumed that the system quantities remain close to nominal frequency, which justifies representing the network by algebraic equations as well as simplifying models

of synchronous machines and other components. These simplifications limit the frequency range of validity of the results obtained, but bring considerable gains in terms of computational effort needed to simulate the system. A general comparison of the software tools is provided in Table 4.

For each of these classes of programs, a specific software was chosen to serve as a case study for the comparison throughout this chapter: PSCAD for EMT simulations and PowerFactory for the RMS simulations. The following section provides an overview of the models recommended in the literature for the interaction studies, with special focus on those suitable for interactions in the frequency range defined previously. The models available for practical use in the two programs chosen are also examined. Further information about the PowerFactory modelling principles and guidelines can be found in [1]-[5] and for PSCAD in [6].

5.2 Power system modelling

The main objective of this section is to illustrate the modelling differences found in the two main classes of programs. This section provides a review of the models found in literature and those found in PSCAD and PowerFactory for some of the main power system components: synchronous generators, transmission lines and converters. It is important to note that in this report only the models typically associated with RMS simulations were considered when reviewing PowerFactory so it could serve as a basis for comparing it to PSCAD which is a typical EMT tool.

5.2.1 Synchronous generators

The synchronous generator models generally recommended for stability analysis range from the simple voltage behind transient reactance model all the way to the sixth-order model where both direct and quadrature axes are modelled by three circuits.

An effort was made to provide a compilation of the main synchronous machine models used in stability studies which was accomplished in the IEEE Guide for Synchronous Generator Modelling [7]. These models are developed in the dq-frame and they are classified according to their order considering each axis individually. These range from one to three, indicating how many circuits are modelled in that axis. Below is a summary of the main models based on the order of the d-axis circuit:

Table 4: Comparison between EMTP and transient stability programs.

	Electromagnetic transient programs	Transient stability programs
Solution method	Instantaneous values of variables are calculated by solving the differential equations	Variables are represented by phasors and sometimes only solved for positive sequence values
Assumptions	No implicit assumptions	Variables do not deviate significantly from nominal frequency
Equation simplifications	No implicit simplifications	Steady-state network equations and simplified machine equations
Frequency range of accuracy	Wide frequency range, depending on choice of models	Only accurate around nominal frequency
Simulation time step	Microseconds	Few milliseconds
Commercial routines	PSCAD, EMTP-RV, RSCAD, ATP, PowerFactory	PowerFactory, PSS/E, Eurostag

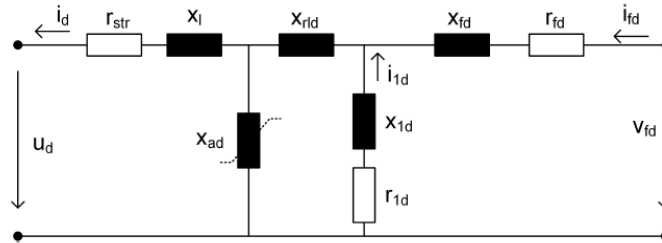


Figure 26: D-axis representation of Models 2.1 and 2.2. [1]

Classical model This model is the simplest available. It consists of a constant voltage source behind a transient reactance. In this model, all electromagnetic dynamics are neglected and the field voltage is considered constant, resulting in a constant electromotive force. It can be used when conducting screening studies to obtain a first idea about the system behavior, to represent generators located far from the point where the disturbance is applied or for machines that have relatively smaller sizes when compared to other machines in the system under study.

First order d-axis models In this model, only the effect of the rotor field winding is present, which leads to a first-order circuit in the d-axis. It is the simplest model to which an automatic voltage regulator can be connected. The q-axis can be either first or second order, depending on whether it models or not the equivalent effect of a damper circuit.

Second order d-axis models This model presents a higher level of modelling detail and is the most common machine model used in transient stability studies [7]. This category includes two models: Model 2.1 and Model 2.2. In both cases the rotor d-axis is modelled by two rotor loops that represent the excitation field winding and the 1d-damper winding as displayed in Figure 26. The main difference between the two is that Model 2.1 has a single 1-q damper winding and is recommended when representing most salient-pole machines while Model 2.2 has two damper windings (1-q and 2-q) and can represent some round-rotor machines such as turbo-generators [7]. Both cases are illustrated in Figure 27.

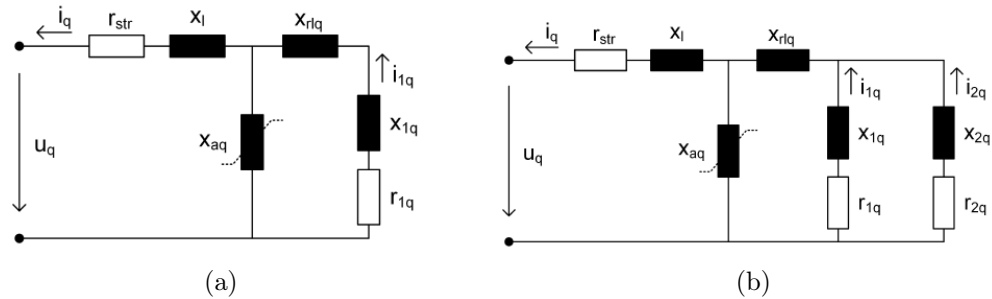


Figure 27: Q-axis representation of (a) Model 2.1 and (b) Model 2.2. [1]

Third order d-axis model In this category, only the structure of Model 3.3 is considered to be of practical use. For this model the rotor d-axis circuit is represented by the excitation field winding and two damper windings (1-d and 2-d). The q-axis circuit is represented by three rotor loops, hence the denomination of the model. Even though higher-order models exist, this model is considered to be the most detailed model needed for most stability studies involving large systems [7].

PSCAD and PowerFactory

PowerFactory offers three models for synchronous machines. These are included in the element *ElmSym*: the classical model, standard model (Model 2.1 and Model 2.2) and Model 3.3. Even though the model structure is very similar to those mentioned above, there are fundamental simplifications made when RMS simulations are concerned. These simplifications are discussed below:

- The transformer voltage terms (derivative of the stator fluxes ψ_d and ψ_q) are neglected, which means that ψ_d and ψ_q are not state variables;
- Available as an option: the effect of rotor speed variation on the stator voltages can be considered, completely neglected or partially neglected (taken into account in only some of the equations).

PSCAD uses a model similar in structure to Model 2.2. In this model, the d-axis equivalent circuit considers two windings: field excitation and damper winding. Similarly, the q-axis circuit includes 2 damper windings to allow the representation of both salient pole and round rotor configurations.

The equivalent machine circuit configuration is very similar when PSCAD and PowerFactory models are compared. However, PowerFactory models makes assumptions regarding the transformer voltage terms and rotor speed variations while the PSCAD model does not.

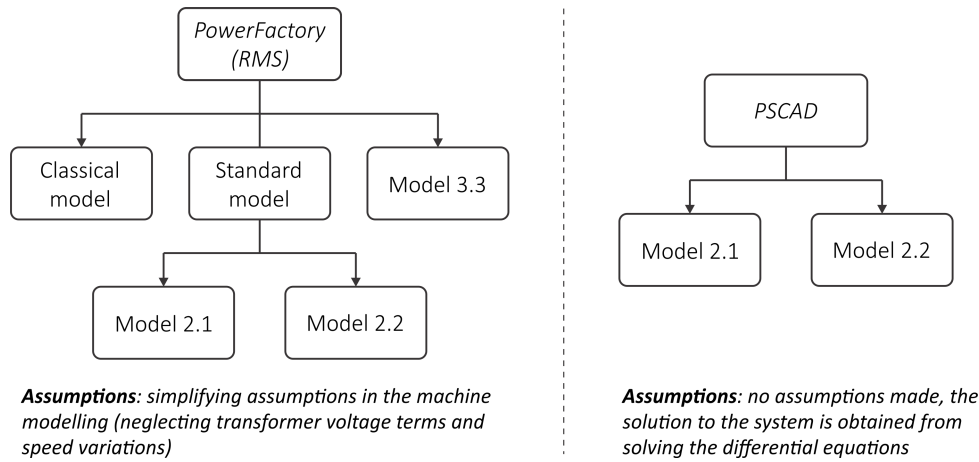


Figure 28: Overview of the synchronous generator models available in PowerFactory and PSCAD.

5.2.2 Converters

Several models are available for converters depending on the frequency range of the phenomena of interest. For the studies of interest in this report, that is, restricted to frequencies close to or slower than the nominal system frequency, it is a common approach to take into account the converter behavior at fundamental frequency, resulting in an averaged model. As an illustration, two model types of modular multilevel converters for AC and DC stability studies are detailed below:

- Averaged Value Model (AVM) based on the switching function: This model assumes that the capacitor voltages are balanced. The AC side is represented by a controlled voltage source while the DC side is represented by a current source, the magnitude of which depends on the power coming from the AC side. This is illustrated in Figure 29. It uses switching functions in order to represent the harmonics generated by the switching devices, but it can only be implemented in EMT tools [9].

- Simplified Average Value Model: This model is similar to the previous one where the converter is modeled as a controlled voltage and current source. However, the switching harmonics are not taken into account.

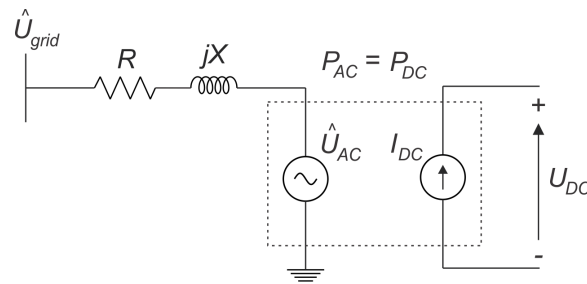


Figure 29: Average Value Model of a VSC converter.

PSCAD and PowerFactory

In terms of converters, the PSCAD library offers a model of a six-pulse bridge used in HVDC line-commutated converter configurations. Other converter topologies can be found in the example cases provided with the software package, but these are typically built using more basic component models such as power-electronic switches. Following the same principle or based on the available examples, the user can implement case-specific custom models. This software allows for both the implementation of simplified up to very detailed models, including switching devices and complex controls.

In PowerFactory there are several ways to model a converter. Some models are directly available as pre-defined components such as the PWM Converter element (*ElmVsc* and *ElmVscmono*) or the rectifier/inverter element (*ElmRec* and *ElmRecmono*). Alternatively, it is possible to implement HVDC systems and renewable energy sources by representing them as a voltage or current sources as shown in Figure 29. This can be done with the element *ElmGenstat* that represents what is called a static generator. In Figure 30, a brief overview is provided for the main models available in PowerFactory and PSCAD.

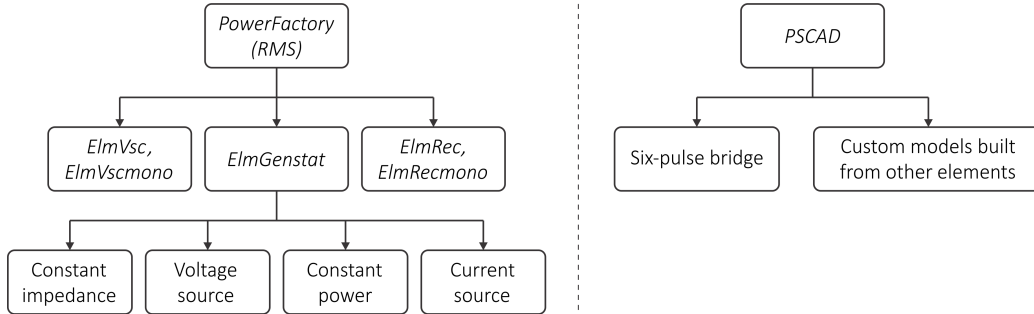


Figure 30: Overview of the models available for converters in PowerFactory and PSCAD.

PWM converter The PWM converter element allows the modelling of both a self-commutated two- or three-level voltage source converters and half-bridge modular multilevel converters. It implements the fundamental frequency model where the converter is represented by an AC voltage source controlled by the DC voltage. The converter equations are predefined and the model typically uses the modulation index as a control input.

Static Generators In RMS simulations, four models are supported by *ElmGenstat*: current source, voltage source, constant impedance and constant power [4]. These models do not implement directly any converter equations. They can be used as basic components to implement some of the more simplified converter models, but all the controls and supporting equations need to be implemented by the user. A summary of these models is provided below.

- Current source model: It represents the converter as a current source determined by the currents to be injected given in the dq frame i_{dref} , i_{qref} and the dq reference angle $cosref$ and $sinref$.
- Voltage source model: It is composed of a voltage source behind an impedance. The inputs that must be provided are the real and imaginary parts of the voltage source $u1r_{in}$ and $u1i_{in}$ as well as the copper losses P_{cu} and short-circuit impedance uk of the series reactor. The reactor impedance is calculated from the last two parameters mentioned.
- Constant impedance model: In this model no inputs are needed. The

converter is represented by a constant impedance which is calculated using the current and voltage obtained from the load flow calculation.

- Constant power model: It represents the converter by a constant active and reactive power injection multiplied by a scale factor. The power and scale factor must be provided as inputs for this model.

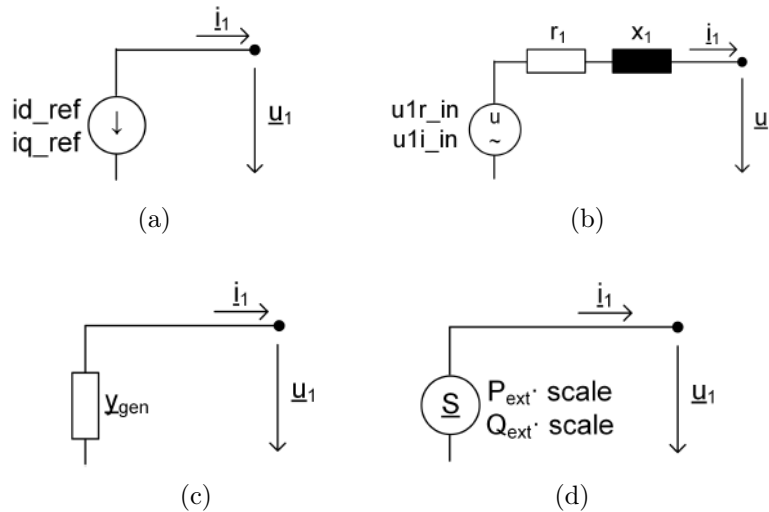


Figure 31: Models supported by the element *ElmGenstat*: (a) current source, (b) voltage source, (c) constant impedance and (d) constant power. [4]

5.2.3 Transmission lines

Transmission line models used in AC system analysis can broadly be classified into lumped- or distributed-parameter models and can be frequency dependant or evaluated at a single frequency. Below a brief description of each type of model is presented.

Lumped-parameter model The lumped parameter model is recommended for short to medium length transmission lines. It is represented by an equivalent PI-circuit where the total line resistance, inductance and capacitance are lumped as if they were located in a single point, ignoring the effects of electromagnetic travelling waves. Parameters are typically evaluated at a single frequency, typically the nominal frequency (50 or 60 Hz).

Distributed-parameter models As opposed to the previous model, the distributed parameter model takes into account the travelling wave effect in the line. This model is generally recommended when representing long lines. Distributed-parameter models can be either frequency-dependant or based on constant parameters (evaluated at the nominal frequency). The frequency-dependant models represent the transmission line over a wide-frequency range. This is achieved by accounting for the variation of the line parameters as a function of frequency. In the constant parameter model, the line parameters are calculated at nominal frequency and the model will be less accurate if the signal has components at other frequencies.

PSCAD and PowerFactory

There are two types of transmission line models available for RMS simulations in PowerFactory, referred to as lumped and distributed parameter models.

The lumped parameter model is recommended for short to medium length transmission lines. It is represented by an equivalent PI-circuit. For a three-phase line, the input parameters are given as the total positive and zero sequence impedances and admittances where the negative sequence is considered to be equal to the positive sequence values.

For long lines, the distributed parameter model can be used. This model is also represented by an equivalent PI circuit, but the impedance and admittance become frequency-dependant parameters since they are written as a function of the line surge impedance and propagation factor [2].

PSCAD offers both lumped and distributed-parameter transmission line models. The lumped parameter model is based on the pi-section similar to what is found in PowerFactory. The distributed-parameter models include both those calculated at a single frequency and those valid at a wide frequency range. These models are described in Section 3.3 and a brief summary is also included below for completeness:

- **PI circuit:** This model represents the line by a series impedance and a shunt admittance and it is only recommended for representing short transmission lines where the propagation delays can be neglected.
- **Bergeron model:** This model is the simplest distributed parameter model available on PSCAD. It represents the line as an infinite sequence of PI sections, but it considers the line resistance lumped at

both ends and at the middle of the line. The model parameters are calculated for a single frequency. Due to that, it is only recommended for studies where frequencies other than the fundamental frequency are not relevant [6].

- Frequency dependant models: The frequency dependant models are solved for a number of frequency points within a frequency range specified by the user. Unlike in the Bergeron model, this model also considers the line resistance to be distributed along the line length, as well as its capacitance and inductance. Two types of models are available: modal domain and phase domain.

Figure 32 provides a summary of the transmission line models available in both PSCAD and PowerFactory.

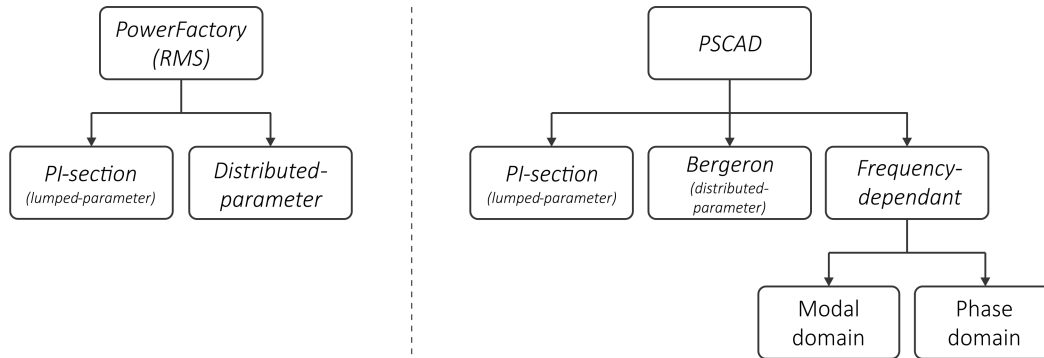


Figure 32: Overview of the models available for transmission lines in PowerFactory and PSCAD.

5.3 Conclusions

The increase of HVDC, renewable energy and FACTS devices in the grid have brought along new challenges to studying power system stability. Traditional transient stability tools classically used to study the stability of large systems was shown to not always be accurate enough. This is because most of the oscillations in classical systems dominated by synchronous machines have been slow and dominated mainly by the machine dynamics. The introduction of power-electronic converters led to new types of interactions that now involve converters and other grid devices, having a frequency content that

is no longer restricted to the range observed in traditional systems. This creates the need to evaluate the limitations of traditional transient stability tools.

This report intended to highlight the main modelling differences between the two types of power system simulation tools: EMTP and transient stability programs. Commercial tools were used as representatives of each of these classes of programs: PSCAD for EMT programs and PowerFactory for transient stability programs. The models recommended in literature were covered for a selection of the main grid components. Their representation in PSCAD and in PowerFactory have been described as an illustration of the typical differences found in modelling a power system for stability studies in these two classes of programs.

References

- [1] DIgSILENT PowerFactory 2017, Technical Reference - Synchronous Machine, 2017.
- [2] DIgSILENT PowerFactory 2017, Technical Reference - Overhead Line Models, 2017.
- [3] DIgSILENT PowerFactory 2017, Technical Reference - Cable System, 2017.
- [4] DIgSILENT PowerFactory 2017, Technical Reference - Static Generator, 2017.
- [5] DIgSILENT PowerFactory 2017, Technical Reference - PWM Converter, 2017.
- [6] Manitoba HVDC Research Center, EMTDC User's guide, 2016.
- [7] "IEEE Guide for Synchronous Generator Modeling Practices and Applications in Power System Stability Analyses," in IEEE Std 1110-2002 (Revision of IEEE Std 1110-1991), pp.1-72, 2003.
- [8] F. Milano, Power System Modelling and Scripting. New York, NY, USA: Springer, 2010.
- [9] W. G. B4.57, "Guide for the development of models for HVDC converters in a HVDC grid," CIGRE, Tech. Rep., 2014.

6 Converter interactions in AC/DC grid operation

Written by Vaishally Bhardwaj, approved by Hakan Ergun and Dirk Van Hertem.

An increasing integration of HVDC into the existing power system and the envisaged large scale development of HVDC grids would add additional degrees of freedom in system control and management [1]. However, such a system of hybrid AC/DC grids may also exhibit various kinds of interactions which may pose new challenges for reliable grid operation. In this section, such interactions between the AC/DC grid converters are presented.

The work is organized into 3 subsections. Firstly, possible converter interactions in multi-zonal AC/DC systems are highlighted. This is followed by the implications of such interactions on overall system operation and on the available flexibility from the converters. In the next section, a tool for computationally efficient implementation of AC/DC security constrained optimal power flow is discussed. Finally, the section is summarized in the conclusion.

6.1 AC/DC converter interactions in multi-zonal systems

In case of interconnected power systems, power flow controlling devices such as the AC/DC converters may not only allow local control of system parameters but also strongly influence the grid flows over a wide area [1][2][3]. When many such devices are considered in the context of multi-zonal (multiple operator) interconnected systems over multiple time frames, they may affect each others' operation. These interactions may either be unintentional, due to a lack of coordination and mutual information sharing, or may be intentional wherein gaming behaviour comes into play. Thus, overall coordination between stakeholders/operators of the different control areas is critical for a holistic and secure operation of the system.

These converter interactions are much slower (in the order of seconds up to minutes) as compared to the "dynamic" time-scale which is characterized by faster power system phenomena. Nevertheless, they impact the optimal operation of a power system constituting multiple control areas.

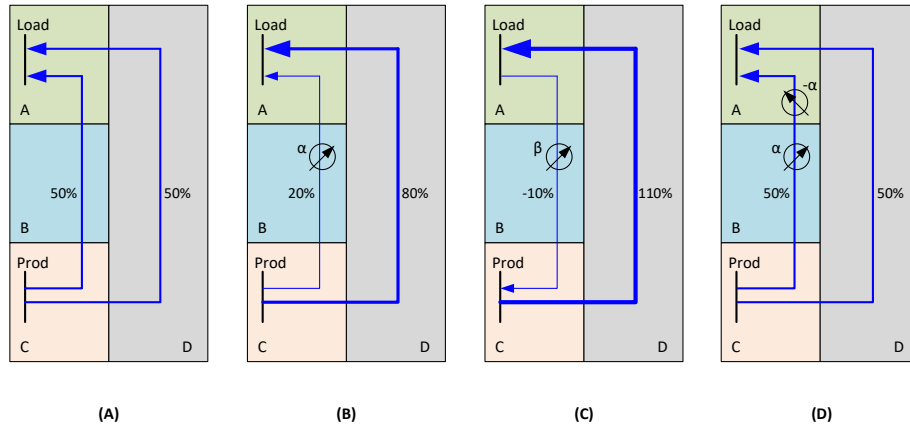


Figure 33: Impact of controlling devices on power system [3].

In order to understand the impact of such converter interactions, a simple 4-zone system as given in Figure 33 is considered. In this system, zone C is characterized by net power production, whereas zone A has a net demand. For the normal scenario (Case A), the power flows from zone C to zone A in the system distribute equally through the two intermediate zones B and D.

Consider the scenario wherein the operator for zone B replaces the existing AC interconnection within the control area with an HVDC interconnection such that the converter settings now limit the flows through this zone to 20%. In such a situation (Case B), the power flows are redistributed through zone D which now accounts for 80% of the flows. While this scenario is beneficial for zone B, it may lead to higher flows in zone D and in worst cases, congestion or voltage issues. As there is no coordination amongst the individual zones, the operator of zone D may also not be aware of the state of the neighbouring grid B.

In another circumstance (Case C), zone B operator may set the converter set points so as to enable a flow of 10% from zone A towards zone C. This would result in even higher flows (110%) through zone D and may culminate in congestion problems. In case of a real system, such a situation may arise when the operator optimizes the converter settings for its control area by considering the local objective, while ignoring the grid situation in neighbouring zones knowingly or unknowingly. It may also be the case when the

converter set points are based on a predetermined load generation scenario of the overall grid which does not correspond with the actual grid situation.

Finally the system state in Case D is considered, where the operator of zone A implements a similar HVDC interconnection such that it counteracts the zone B converter settings and leads to changed power flows as compared to Case B. Thus, it is seen that the converter set points influence the system flows largely (active power flows as well as reactive power flows). Moreover, with no coordinated control, each operator tries to find the most optimal converter set points with respect to their individual control area. These set points might lead to sub-optimal or inefficient operational state for the overall system.

Within the purview of short-term grid operation [4], the grid operator performs a security-constrained optimization based on the submitted bids in the D-1 or day ahead market in order to identify the hourly dispatch for the next day. For the intra-day operations, the same approach is utilized for determining the most optimal set points of the controllable devices for the next hour/s. When the operation of a hybrid AC/DC multi-zonal system is not synchronized, every operator may carry out its individual security assessment to obtain the most optimal set points for its converters at a particular time step. As the converter set points may affect the overall grid flows in actual operation and lead to sub-optimal operation in another control area, one or more of the operators may need to carry out a re-dispatch in the next time step for countering the unexpected flows and finding an optimal operational state for their respective control areas. This may lead to direct or indirect interactions between the converters of different control areas of a large interconnected AC/DC system over the multiple time frames of grid operation [4]. Thus, it is imperative that effective coordination and transparency is needed among the operators for a cost-effective and reliable operation of the overall system.

It has been seen in [4][5], that the characteristic controllability of HVDC systems could be utilized in order to alleviate system uncertainties and operate the system much closer to its limits. As the time response of the AC/DC converters is much faster as compared to the traditional control devices of the AC system e.g. phase shifting transformers, they could be employed for fast corrective control measures in case of a system contingency. This would enable an extension in the system operating boundary as seen in Figure 34(ii).

In case a contingency occurs, the predetermined control action from the converters gets activated and the system operating point is brought back into

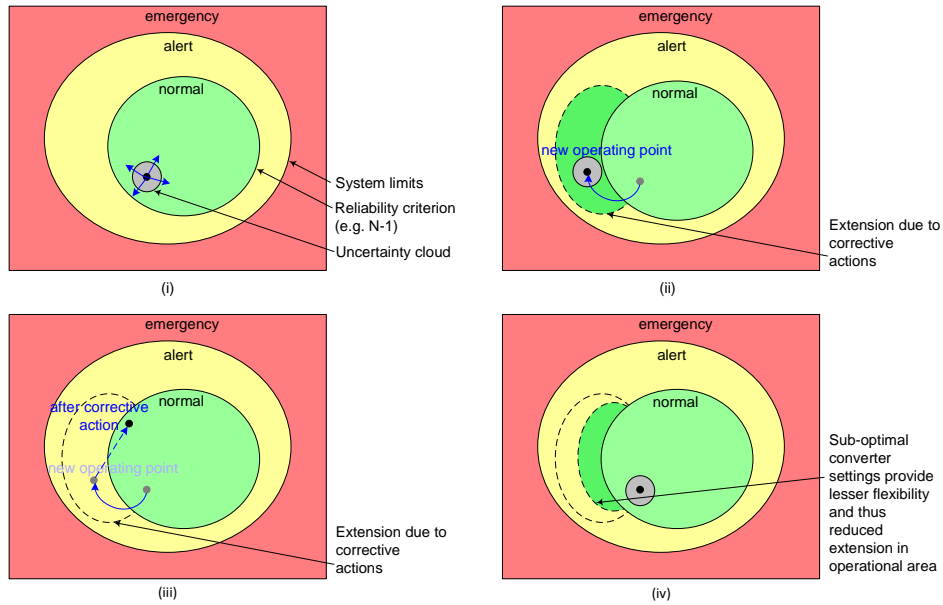


Figure 34: Flexibility in system operation through AC/DC converters[6]

the "normal" zone as seen in Figure 34(iii). Such a flexible and fast control would facilitate the operation of the system at the most optimal state with minimum risk.

However, this would hold true only for a system with adequate coordination among its individual control area operators. In the absence of such integrated and coordinated control, the operators may not operate the converters as per the most optimal state for the overall system and this may in turn reduce the flexibility in some measure as compared to that in case of coordinated optimization and dispatch. This effect can be visualized in the reduced extension of flexible operating area in Figure 34(iv).

6.2 Computationally efficient implementation of AC/DC security constrained optimal power flow

It is evident that controlling the converters locally in a meshed and multi-zonal AC/DC system may lead to problems in the individual zones and inefficient operation of the global system. In order to analyze the above discussed converter interactions for such a hybrid AC/DC system over different

time frames, a multi-stage security constrained optimization needs to be performed. Eventually, a framework for the coordinated operation of such an AC/DC grid needs to be envisaged. This is a non-convex, non-linear, large-scale optimization problem with many control variables and belongs to the class of mixed integer non-linear problems. As with non-convex optimization, there exists the problem of obtaining either a local optimal solution within less time or the vice-versa, it would be expected to implement some convex relaxations or approximations of the actual non-linear problem that guarantee a global optimal solution (of the relaxed problem) within acceptable computational time. It would also be crucial to establish a comparative analysis of the proposed relaxations with each other as well as with respect to the classic non-convex, non-linear AC problem.

While there are many emerging methods and formulations in the literature [7] for solving power system optimization problems such as the linear programming approximation for AC power flows (LPAC), linear approximation in rectangular coordinates (LACR), Semidefinite Programming (SDP), Quadratic Convex (QC), Second Order Cone (SOC), etc., it is observed that these implementations are complex mathematical models and are based on a variety of optimization softwares. These softwares are utilized through an interface layer of different modeling languages such as AMPL, GAMS, OPL, Pyomo and YALMIP. Thus, it is challenging to benchmark the developed formulations on the same level and evaluate them for solving wide variety of power system optimization problems.

Over the last few years, the platform of Julia and JuMP is gaining popularity for implementing mathematical optimization problems. Julia is an open-source, high-level, high-performance programming language used for numerical computing. Owing to its free and open-source environment, Julia presents a good alternative to many other modeling languages such as MATLAB-based MATPOWER and provides the flexibility to introduce new packages for a variety of computations. JuMP is one of the open-source packages embedded in Julia which is used for solving mathematical optimization problems. It supports a number of open-source and commercial solvers such as Cbc, Clp, CPLEX, Gurobi, Ipopt, MOSEK, SCS, etc and could be used for solving a diverse array of problem classes.

Based on the platform of Julia and JuMP, an open-source toolbox of PowerModels has been implemented [7] which reflects the structure of power system mathematical programs. This package can be used to solve various power system problems e.g., Power Flow, Optimal Power Flow (OPF), Op-

timal Transmission Switching (OTS) and Transmission Network Expansion Planning (TNEP) through complex formulations that are based on different approximations and relaxations. One of the key highlights of this package is the decoupling between the power system problem specification and the system formulation, which allows to compare the results of undertaking the same optimization problem while using different formulations.

Further on top of the PowerModels modeling layer, two more packages have been developed namely PowerModelsACDC [8] and PowerModelsReliability [9]. While PowerModelsACDC is an extension package focussed on inclusion of models for DC lines, meshed DC networks, and AC/DC converters, the PowerModelsReliability package is based on power system reliability management through security-constrained OPF. As the concerned problem involves the security-constrained optimization of a hybrid AC/DC system, the ecosystem of PowerModels and its extension packages are being utilized to implement such a problem specification and carry out the further analysis. A steady state representation is used for modelling the DC branch and the AC/DC converter station in the security-constrained optimal power flow. The detailed modelling of the components and the power flow formulation are described in [4].

6.3 Conclusion

It has been seen that the controllability of the AC/DC converters may have dominant influences on the overall operation of the hybrid grid. Thus, these effects need to be properly incorporated while carrying out system reliability assessments at every time step of grid operation. For an optimal and reliable operation of the global system, it would be critical to ensure regular international coordination and transparency among the grid operators. In the absence of such a mechanism, the individual control areas would adhere to local objectives and lead to counter-productive effects in other areas of the system. In order to enable cost-effective operation for the overall system, optimization tools need to be utilized which can provide solutions to such a complex problem with a sufficient accuracy and within reasonable computational time.

References

- [1] Van Hertem, D., Rimez, J. and Belmans, R., “Power Flow Controlling Devices as a Smart and Independent Grid Investment for Flexible Grid Operations: Belgian Case Study”, IEEE Transactions on Smart Grid, Vol. 4, No. 3, pp.1656-1664, September 2013.
- [2] Van Hertem, D., Eriksson, R., Söder, L. and Gandhari, M., “Coordination of multiple power flow controlling devices in transmission systems”, 9th IET International Conference on AC and DC Power Transmission (ACDC 2010), London, UK, October 2010.
- [3] Van Hertem, D., Verboomen, J., Cole, S., Kling, W.L., and Belmans, R., “Influence of phase shifting transformers and HVDC on power system losses”, IEEE Power Engineering Society General Meeting 2007, Tampa, Florida, USA, June 2007.
- [4] "Deliverable 3.1–Work Package 3:Report on the review and evaluation of DC and AC grid operation and interactions in different time frames.", Innovative tools for offshore wind and DC grids (InnoDC), Available at: https://mappedsites.cardiff.ac.uk/innodc/wp-content/uploads/sites/11/2018/10/201808_WP3_DCAC_Grid_Operation_Interactions.pdf.
- [5] Van Hertem, D., Gomis-Bellmunt, O., Liang, J., "HVDC Grids For Offshore and Supergrid of the Future", Wiley IEEE Press, February 2016.
- [6] Van Hertem, D., "Reliable power system operations with hybrid AC/DC grids", ICEE Seoul, 2018.
- [7] Coffrin, C., Bent, R., Sundar, K., Ng, Y. and Lubin, M., "PowerModels.jl: An Open-Source Framework for Exploring Power Flow Formulations", Power Systems Computation Conference (PSCC) 2018, Dublin, June 2018.
- [8] Ergun, H., Dave, J., Van Hertem, D., Geth, F., "Optimal Power Flow for AC/DC Grids: Formulation, Convex Relaxation, Linear Approximation and Implementation", IEEE Transactions on Power Systems, February 2019
PowerModelsACDC.jl package Available at: <https://github.com/hakanergun/PowerModelsACDC.jl>.

- [9] PowerModelsReliability.jl package Available at: <https://github.com/frederikgeth/PowerModelsReliability.jl>.